Binding Energies in Atomic Negative Ions

H. Hotop

Fakultät für Physik, Universität Freiburg, Freiburg, Germany

and

W. C. Lineberger

Joint Institute for Laboratory Astrophysics, University of Colorado and National Bureau of Standards

and

Department of Chemistry, University of Colorado, Boulder, Colorado 80302

A survey of the electron affinity determinations for the elements up to $Z = 85$ is presented, and based upon these data, a set of recommended electron affinities is established. Recent calculations of atomic electron affinities and the major semiempirical methods are discussed and compared with experiment. The experimental methods which yield quantitative electron binding energy data are described and intercompared. Based primarily upon extrapolation techniques, fine structure splittings for these ions and excited state term energies are given.

Key words: Ab initio calculations; atomic negative ions; binding energy; electron affinity; excited states; experimental methods; fine structure splitting; recommended values; semiempirical calculations.

Contents

List of Tables

539

J. Phys. Chem. Ref. Data, Vol. 4, No. 3, 1975

Abbreviations

IE	Isoelectronic extrapolation	HA	Horizontal analysis extrapolation
HF	Hartree Fock	VA	Vertical analysis extrapolation
MC	Multiconfiguration(al)	SSI	Self-surface ionization
CI	Configuration interaction	FIS	Field ionization spectrum
PT	Photodetachment threshold (conventional light source)	SE	Semiempirical extrapolation
		SOC	Superposition of configurations
LPT	Laser photodetachment threshold	PlA	Plasma absorption (photodetachment)
LPES	Laser photodetachment electron spectrometry	PlE	Plasma emission (radiative attachment)
SI	Surface ionization	IPF	Ion-pair formation by photoabsorption
E_C	Correlation energy		

Preface

In reading review articles, one sometimes gets the impression that all the important advances have been made in the past few years, and that the early work has been totally superseded. Such is certainly not the case in this area, where almost all of the new results and ideas were anticipated and appreciated by the pioneers in the study of electron binding to atoms. In this spirit, we dedicate this review to Lewis M. Branscomb, who truly gave birth to quantitative studies of photon-negative ion interactions. Virtually all of the new experimental results reviewed here were anticipated by him, and would have been produced by him, had present laser light sources been available a few years earlier.

1. Introduction

The use of both fixed frequency and tunable laser light sources in negative ion photoabsorption studies [1–15] [1] and the recent progress in ion source technology [e.g. 16–18] have resulted in major improvements in our knowledge of binding energies in many atomic [2, 3, 7–10, 14, 15, 19, 20] and some molecular negative ions [4–6, 11–13, 21] over the past few years. This article summarizes this progress and discusses in some detail the laser photodetachment techniques. Other experimental methods which have produced quantitative

electron binding energy data are presented in somewhat less detail, and an attempt is made to assess the accuracy of all experimental methods employed to date. Based upon this discussion, a summary of atomic electron affinity determinations is given, and a compilation of recommended electron affinities for elements with $Z \leqslant 85$ is provided. Recent calculations of atomic electron affinities and the major semiempirical extrapolation methods are discussed and compared with experiment. Based mainly upon extrapolations, values for fine structure intervals in atomic negative ions are given.

There have been a number of excellent reviews of our knowledge about negative ions, including those by Massey [22], Pritchard [23], Buchel'nikova [24], Branscomb [25], Moiseiwitsch [26], Smirnov [27, 28], Vedeneyev et al. [29], Smith [30], Page and Goode [31], Berry [32], and Steiner [33]. The review by Steiner [33] provides a thorough entry to the literature prior to 1970. Since the publication of these reviews, however, the state of our knowledge of electron affinities, both experimentally and theoretically, has changed significantly, and it is appropriate now to update and summarize this knowledge. Franklin and Harland [34] have recently completed an article on "Gaseous Negative Ions" which strongly emphasizes the current knowledge about *molecular* negative ions but only incorporates a brief description of the progress brought about by laser photodetachment, in particular in the subfield of atomic negative ions. Popp [35] has just published an extensive

---

[1] Figures in brackets indicate literature references at the end of this paper.

review, "Radiation of Atomic Negative Ions," which provides a unified, thorough discussion of the various plasma techniques.

This review will be limited to those negative ions which, by virtue of their *positive* electron affinity, are stable, and those negative ions which have a negative electron affinity with respect to the ground state but whose lifetime is longer than about 10^{-6} s. The latter class of negative ions live long enough to be detectable in a mass spectrometer, just like the stable negative ions.

Excluded from this review are negative ions whose electron affinity is negative and which have lifetimes shorter than 10^{-6} s. These negative ions are detected as resonances in electron scattering, and they have been recently reviewed by Schulz [36, 37]. Their ground state lies in energy above the ground state of the corresponding neutral atom, and thus they can emit the extra electron spontaneously, with a lifetime which may be as short as 10^{-15} s. These "resonances" may be indicative of the ground state of the negative ion or of higher excited states. Despite the difference in methods of detection, there is a continuous transition between ions whose electron affinity is negative and those whose electron affinity is positive.

In the past few years, there have been reports from several laboratories [38, 39] concerning the observation of long-lived doubly-charged negative ions, e.g., F^{--}, but there has not been much success in duplicating these results in other laboratories [210, 211]. Since the existence of these ions is not certain we shall discuss them only briefly. A short-lived (10^{-15} s) H^{--} ion, has, however, been observed by Walton, et al. [42], as a resonance in $e - H^{-}$ scattering; calculations by Taylor and Thomas [43] using the resonance stabilization methods corroborate this identification.

The published literature has been searched through May 1975. The principal sources of literature have been Physics Abstracts, Chemical Abstracts, the Atomic Collision Cross Section Information Center at JILA, and previous reviews. In an attempt to keep the bulk of literature to a manageable size, we have somewhat arbitrarily excluded a number of types of papers from the bibliography. Since the subject of this review is binding energies, we have excluded calculations of photodetachment cross sections which do not provide new information on electron affinities. An example of such a calculation would be a photodetachment cross section calculation using a Hartree-Fock negative ion wave function. Since accurate calculations of electron affinities are essentially accurate calculations of correlation energies, we have excluded calculations which do not go beyond (restricted) Hartree-Fock. Many early experimental studies of negative ions were qualitative in the sense that a positive binding energy for the extra electron was deduced from the observation of the negative ion in a beam machine. If such qualitative observations have been superseded by quantitative measurements,

then we have excluded the early observations.

In the remaining sections of this review we will discuss the major theoretical techniques for computation of electron binding energies (section 2), semiempirical methods (section 3), the major experimental techniques for determining electron binding energies (section 4), excited levels of negative ions (sections 5 and 6), and provide a summary of the "best" electron affinities available at present. The discussion of theory will be from an experimentalist's point of view and will include semiempirical methods. The section on experimental techniques will discuss each of the methods currently being used to provide quantitative electron affinities, and attempt to assess their accuracy in favorable cases. This discussion will be separated into direct and indirect methods.

2. Calculation of Atomic Electron Affinities

The electron affinity EA of an atom A is the difference between the total energies (E_{tot}) of the ground states of A and its negative ion A^{-}:

$$EA(A) = E_{tot}(A) - E_{tot}(A^{-}). \qquad (1)$$

By ground state, one implies the lowest energy fine-structure level, if there is a non-zero spin-orbit interaction. The quantity EA, sometimes called the zeroth ionization potential, is positive if a stable negative ion exists. The total energy can be written as

$$E_{tot} = E_{HF} + E_C + E_{SO} + \delta, \qquad (2)$$

where E_{HF} corresponds to the (restricted) Hartree-Fock energy, E_C is the correlation energy describing the deviation of the many-electron system from the Hartree-Fock (HF) self consistent field model, E_{SO} is the spin-orbit energy for states with nonzero orbital angular momentum and spin, and δ comprises several correction terms [mass polarization, relativistic and radiative effects (Lamb shift)]. Although the Hartree-Fock energy accounts for most of the total energy (e.g., $E_{HF}/E_{tot} \gtrsim$ 99.5% for atoms with $Z = 5-9$) [44-46], the correlation energy is found to play a decisive role in the formation of negative ions. For atomic number $Z < 10$, only carbon and fluorine are predicted to form stable negative ions within the (restricted) HF model [44, 45]; both of these negative ions have closed (sub) shells. Even in these two cases more than half of the energy stabilizing the negative ion arises from the change in correlation energy upon addition of the extra electron [44, 45, 47-49]. Therefore, given HF energies (which are well known [e.g., 44-46, 50-53]), the task of calculating electron affinities is essentially that of obtaining an accurate number for the correlation energy difference, $E_C(A) - E_C(A^{-})$.

The simplest negative ion is, of course, H⁻. Although not analytically solvable, since it is a three-body problem, the H⁻ system is sufficiently simple to allow the use of very elaborate correlated wave functions in a variational calculation of the eigenenergy [54–58 and references therein]. For no other negative ion have calculations of this sort been carried out to convergence; instead various approximate methods have been used to calculate the correlation energy.

In the remainder of this section we will discuss the state of calculations on H⁻, the alkali-metal negative ions, the first row negative ions, and the heavier negative ions.

2.1. The H⁻ Ion

The hydrogen negative ion H⁻ is not bound with the Hartree-Fock approximation $(E_{HF}(H) - E_{HF}(H^-) = -0.328$ eV) [59]. The correlation energy in H⁻ $(-1.083$ eV) [59] stabilizes the negative ion and is a large fraction (7.5 percent) of the total non-relativistic energy in H⁻ $(-14.348$ eV) [56, 57]. Pekeris has carried out very extensive Hylleraas-type variational calculations on two-electron systems [56, 57]. The reader is referred to his papers for a detailed appreciation of his results for H⁻ as well as references to the earlier literature devoted to the same subject.

More recently Aashamar [58] used Hylleraas-Scherr-Knight variational perturbation wave functions, known through 20th perturbation order, to evaluate energies in two electron systems, including lowest order relativistic and radiative corrections. The major results of Pekeris [56, 57] and Aashamar [58] obtained for H⁻ and He are compared [2] with experiment in table 1. We note that there is excellent agreement for He, whereas for H⁻, the two calculated values for EA differ by 0.04 cm⁻¹, primarily as a result of differing non-relativistic energies. This discrepancy can hardly be attributed to an error in Pekeris' calculation for $E_{non-rel}$, in which convergence

---

[2] For reasons of convenience and consistency, energy comparisons in this paper are frequently made in cm⁻¹ units, where 1 eV $\triangleq$ 8065.479(21) cm⁻¹ [214].

down to the 0.001 cm⁻¹ level was demonstrated [57]. The main source of error in the Pekeris calculation for EA(H) is due to the uncertainty in the relativistic and Lamb-shift corrections [56, 57]. It would appear that these corrections are in error by no more than 0.02 cm⁻¹. If one includes the hydrogen atom hyperfine splitting (0.0474 cm⁻¹) and defines the electron affinity as the energy difference between H(F=0) and H⁻(F=1/2), one obtains EA(H) = 6083.06(2) cm⁻¹ $\triangleq$ 0.754209(3) eV. Subsequently we shall ignore the effect of hyperfine structure on electron affinities.

The H⁻ ion occupies a unique niche in this review, for EA(H) is considered to be known theoretically to at least three more significant figures than are obtained from the best experimental determinations. Moreover, the calculated EA(H) is perhaps 100 times more accurate than any experimental determination of an EA. For no other atom is this the case, and it is clear that an experiment that really tests the Pekeris calculations would be valuable.

2.2. Alkali Negative Ions

Most calculations of the EA of alkali atoms have taken advantage of the approximate two-electron nature of the alkali negative ions, i.e., that most of the correlation energy is contained in a calculation of the $(ns)^2$ pair-correlation energy. This approximation naturally becomes worse for heavier alkalis, where the interaction between the outer electron(s) and the core becomes progressively more important. This fact can be seen from the results given in table 2. The CI calculations on light alkalis by Weiss [59, 61], by Fung and Matese [62] and by Grün [63], which yield the $(ns)^2$ pair-correlation energies with high accuracy, are found to be in good agreement with the recent experimental determinations by Patterson et al. [14]. The results of various pseudopotential (or model potential) calculations [64–72] are also generally in good agreement with experiment. For these calculations the core is represented by a suitably chosen effective potential and the two-electron problem is solved with this potential. The effective potentials are

---

TABLE 1. Contributions to EA(H) and IP(He)[a]

	H⁻		⁴He	
	EA$_{non-rel}$	E_{tot} = EA(H)	IP$_{non-rel}$	E_{tot} = IP(He)
Pekeris	6087.328	6083.09	198317.375	198310.68 ± 0.03
Aashamar	6087.38	6083.13	198317.38	198310.69
Experiment		⩾6081 ± 2.5[b]		198310.75 ± 0.12[c, d]

[a] All values are in cm⁻¹ units (1 eV $\triangleq$ 8065.479 cm⁻¹).

E_{tot} contains corrections due to mass polarization, relativistic effects and radiation effects (Lamb Shift). Conversions used are R_H = 109677.577 cm⁻¹ and R_{He} = 109722.267 cm⁻¹. Hyperfine splitting in H was not taken into account.

[b] P. M. Dehmer and W. A. Chupka, Bull. Am. Phys. Soc. 20, 729 (1975).

[c] G. Herzberg, Proc. Roy. Soc. A248, 309 (1958).

[d] M. J. Seaton, Proc. Phys. Soc. 87, 337 (1966).

TABLE 2. Summary of experimental (E) and theoretical (T) values for electron affinities of the alkali atoms (eV)[a]

Author	Method	EA in eV [b]				
		Li	Na	K	Rb	Cs
Weiss [59, 61]	CI pair-correlation (T)	0.62	0.54	0.47	0.42 [c]	0.39 [c]
Fung and Matese [62]	CI pair-correlation (T)	.613	.536			
Grün [63]	CI pair-correlation (T)	.614				
Clementi et al. [44, 50, 51]	HF and EC extrapolation estimates (T)	.58(5)	.78(6)	.90(5)		
Szasz [64]	Pseudopotential (T)	.43	.53	.49	.43	.42
Schwarz [68]	Model potential (T)	.62	.54	.51	.48	
Szasz and McGinn [65]	Pseudopotential with correlated pair wave functions (T)	.57	.49	.55	.52	
Victor and Laughlin [69, 70]	Pseudopotential (T)	.591(6)	.526			
Cavalieri et al. [71]	Model potential (T)		.535	.494	.430	.424
Norcross [66]	Closed-channel scattering (T)	.615	.543	.504	.488	.464
Kancerivicius [73]	Multiconfiguration HF (T)	.602	.462			
Bydin [74]	Resonant charge exchange (T)		$.41\left(^{8}_{6}\right)$	$.22\left(^{8}_{6}\right)$	.16(6)	.13(7)
Smirnov [27, 28]	Reevaluation of Bydin data (T)		.35	.30	.27	.23
Ebinghaus [75]	Dissociative e⁻ attachment (E)	.4(2)	.34(20)	.55(20)	.63(20)	.58(20)
Ya'akobi [76]	Exploding wire plasma (E)	~ .6				
Scheer and Fine [77]	Surface ionization (E)	.85(20)				
Schmidt-Böcking and Bethge [78]	Heavy particle detachment (E)	.56(4)				
Feldmann et al. [20]	Photodetachment threshold (E)	.61(5)	.53(5)	.50(5)	.48(5)	.47(5)
Patterson et al. [14]	Dye laser photodetachment (E)		.543(10)	.5012(5)	.4860(5)	$.4715\left(^{5}_{20}\right)$
Kasdan et al. [14, 19]	Laser photodetachment electron spectrometry (E)	.620(7)	.548(4)		.486(3)	.470(3)
Kaiser et al. [79]	Photodetachment threshold (E)	.611(20)	.539(20)	.497(20)	.490(20)	.470(20)

[a] Semiempirical extrapolation data are discussed separately.

[b] Numbers in parentheses are uncertainties in last digit given, as determined by the individual authors.

[c] Extrapolated from calculations for light alkalis.

normally adjusted to give agreement with the one-electron spectra of the neutral species. It has been noted [71] that the energy results for the two-electron systems are rather insensitive to the form of the trial wave function, so long as the one-electron model potential is well constructed. On the other hand, accurate correlated wave functions may compensate for the inaccuracy of the one-electron model potentials [65, 71]. From the results in table 2 one sees that the agreement is generally poorer for Rb and Cs, which is not surprising in view of the above remarks.

The good agreement with the experiment obtained by Schwarz [68] for K and, in particular for Rb, may be fortuitous, as pointed out by Norcross [66a], in view of the neglect of the so-called "dielectric correction term," which is a correction term to the model potential to account for interaction between the dipoles induced in the core of the two outer electrons.

The calculations by Clementi et al. [44, 50, 51] involve precise determinations of the Hartree-Fock energies in the atom and negative ion, together with an *estimate* of the negative ion correlation energy, the estimate being obtained by extrapolation from isoelectronic atoms and positive ions, as will be described in more detail below. The results reported by Clementi for Na

[50] and K [51] do not agree well with experiment. Although it will be seen later that Clementi's results for most of the other first and second row atoms [44, 50] are in fair to good agreement with experiment, it appears that, on the whole, the uncertainty estimates quoted by Clementi et al. [44, 50, 51], were somewhat optimistic.

An interesting approach to calculating alkali electron affinities has been recently employed by Norcross [66a]. He used the coupled equations of electron-alkali scattering theory with all channels closed and solved the so-defined eigenvalue problem using semiempirical model potentials to represent the core. His results [66b] for the electron affinities of the alkalis are in excellent agreement with experiment. Norcross found that the polarization correlation correction (dielectric term) makes a significant contribution (10 to 20 percent) to the electron affinities of K, Rb, and Cs. Recent pseudo-potential calculations by Bardsley [72] support this finding.

2.3. Ab Initio Calculations of Electron Affinities of B, C, N, O, and F

In this section we discuss and compare ab initio calculations made over the past few years on the open

shell atoms B, C, N, O, F, and their negative ions [47–49, 73, 80–89].

Since the problem of calculating an electron affinity amounts essentially to calculating accurately the correlation energy difference between an atom and its negative ion, the most meaningful comparison with experiment is with an "experimental" correlation energy difference. This quantity is determined using experimental electron affinities as follows. Rearranging eqs (1) and (2), one obtains

$$E_C(A) - E_C(A^-) = - [E_{HF}(A) - E_{HF}(A^-)]$$
$$+ [EA(A) + \{E_{SO}(A^-) - E_{SO}(A)\}]$$
$$+ [\delta(A^-) - \delta(A)]. \qquad (3)$$

The first bracketed term, the Hartree-Fock energy difference, is accurately known, e.g. from Clementi et al. [44, 45]. The second bracketed term corresponds to the "effective" EA, i.e., the energy difference between the statistically weighted centers of the atom and negative ion multiplet terms. This "spin orbit corrected" electron affinity (EA$_{SOC}$) is readily obtained from the experimental EA's, together with measured or extrapolated spin-orbit splittings. For these light atoms, $\delta(A) \cong \delta(A^-)$;

thus the third term contributes negligibly to the correlation energy differences, and

$$\{E_C(A) - E_C(A^-)\}_{exp}$$
$$= - [E_{HF}(A) - E_{HF}(A^-)] + EA_{SOC}. \qquad (4)$$

A comparison between "experimental" and calculated correlation energy differences is presented in table 3, part a giving the "experimental" values, and part b showing calculated correlation energy differences. The "experimental" correlation energy differences shown in table 3a were obtained by using the experimentally determined EA's for B, C, O, and F given in table 10. The N$^-$(^{3}P) ground state is very probably unstable; i.e., N(^{4}S) has a negative EA which was taken, according to the presumably best predictions, to be about -0.07 eV (see section 6) but is included in table 3 for comparative purposes. The atom correlation energies in table 3a, $E_C(A)$, were taken from Veillard and Clementi ([53] as cited in ref. [87]) and should be accurate to better than 1 percent.

The results obtained reflect the substantial difficulty involved in obtaining reliable theoretical numbers for the EA of the small atoms without making reference to experimental data. The current status of such calcula-

TABLE 3a. "Experimental" correlation energy differences between first row atoms and their negative ions. (All energy values in Hartrees; 1 Hartree = 27.210 eV.)

	B(^{2}P) − B$^-$(^{3}P)	C(^{3}P) − C$^-$(^{4}S)	N(^{4}S) − N$^-$(^{3}P)	O(^{3}P) − O$^-$(^{2}P)	F(^{2}P) − F$^-$(^{1}S)
Calculated					
−E$_{HF}$(A) [44, 45]	24.5291	37.6886	54.4009	74.8044	99.4093
−E$_C$(A) [53, 87]	.1247	.1565	.1886	.2579	.3220
E$_{HF}$(A) − E$_{HF}$(A$^-$) [44, 45]	−.0099	.0202	−.0790	−.0199	.0501
Experimental					
EA$_{SOC}$	.0103(4)	.0467(2)	−.0025	.0538(1)	.1256(1)
"Experimental"					
E$_C$(A) − E$_C$(A$^-$)	.0202	.0265	.0765	.0737	.0755

TABLE 3b. Calculated correlation energy differences, $E_C(A) - E_C(A^-)$.

Authors and Method	B(^{2}P) − B$^-$(^{3}P)	C(^{3}P) − C$^-$(^{4}S)	N(^{4}S) − N$^-$(^{3}P)	O(^{3}P) − O$^-$(^{2}P)	F(^{2}P) − F$^-$(^{1}S)
Clementi and McLean [44] (HF+E$_C$ extrapolation)	0.021(2)	0.023(2)	0.069(4)	0.065(5)	0.074(3)
Moser and Nesbet [47] (Bethe-Goldstone, orbital excitations) one and two particle terms	.0242	.0335	.086	.0956	.1025
Moser and Nesbet [47] (including three particle terms)	.0182	.0273	.0746	.0725	.0727
Weiss, et al. [80, 81] (symmetry-adapted pair correlation)				.075	.078
Sasaki and Yoshimine [49] (CI including single and double excitations)	.0147	.0198	.0552	.0561	.0588
Sasaki and Yoshimine [49] (CI including single through quadruple excitations)	.0156	.0207	.0599	.0613	.0645

tions is thoroughly discussed in a paper by Sasaki and Yoshimine [87], who have carried out very extensive CI calculations of these atoms and their negative ions [49]. These authors have been able to obtain about 95 percent of the correlation energy for both atoms and negative ions, and yet a comparison of their EA's with experiment shows that they have obtained only about 80 percent of the correlation energy of interest (i.e. their numbers for $E_C(A) - E_C(A^-)$ are about 4/5 of the "experimental" values; see table 3).

Table 3 gives a quantitative feeling for the importance of the correlation energy for negative ion formation if one compares the quantity $E_{HF}(A) - E_{HF}(A^-)$ with $E_C(A) - E_C(A^-)$. At the same time a comparison of the "experimental" correlation energy differences with ab initio calculations by Moser and Nesbet [47] by Weiss et al. [80, 81] and by Sasaki and Yoshimine [49] emphasizes the difficulties encountered in these calculations. The problem is, of course, to obtain reliably that part of the correlation energy that is responsible for negative ion formation. Since one is forced to use a limited basis set, a good physical choice of the basis and of the subsequent procedure is essential to get good answers. It is clear that the value of a particular procedure can in effect only be assessed by a comparison of the results with reliable experimental data. In this sense we believe that the calculation of electron affinities of open shell systems is an improtant testing ground for the various approaches to calculating correlation energies.

Pair-correlation is known to contain the major contribution to the lowering of the total energy below the HF value [47-49, 80-82, 84, 85]. Various pair-correlation approximations have been applied to the calculation of EA's [47-49, 59, 61, 80-82, 84, 85]. Of these pair-correlation approximations, the symmetry-adapted pair method used by Weiss et al. [81, 82] is of particular interest since it gives very good results (see table 3) with a relatively small orbital basis set, and without explicitly taking into account the effects of electron excitations higher than double. It is known that the pair-correlation approximation generally overshoots the total correlation energy if a complete orbital basis set is used [49, 87, 90-92]; i.e the sum of pair energies exceeds the "true" correlation energy as shown, for instance, for the L-shell in neon by Nesbet et al. [90]. In that case one has to take into account pair-pair interaction, in order to reduce the deviation from the "true" limit. This means that the success of the calculations by Weiss et al. [80, 81] is in part due to the cancellation of various terms, thereby yielding just about the right correlation energy difference with a limited basis set. Sasaki and Yoshimine [49] have investigated this point in some detail; they conclude that the symmetry-adapted pair-approximation would over-estimate the EA if a complete orbital basis set is used. The "dielectric corrections" of Norcross [66a] behave in much the same manner. The correction "overshoots" if a complete set of outer electron correlations is employed, and then drops back down [66b]

when excited core configurations are added.

Upon inspection of the correlation energy differences in table 3a, one notices the following interesting behavior: $E_C(A) - E_C(A^-)$ is rather small and similar in absolute value for $Z = 5$, 6, and then charges abruptly to a new, nearly constant, three times higher value for $Z = 7, 8, 9$. For the second row, we note that the behavior is similar, except that the absolute values of the differences $E_C(A) - E_C(A^-)$ are about 2/3 of the corresponding ones in the first row. This regularity is also reflected in all the calculated values listed in table 3b. The change in correlation energy upon addition of a p-electron appears to be small as long as empty orbitals are available, but much larger when spins are being paired. This effect can be viewed in terms of the Exclusion Principle. For parallel spins a Hartree-Fock model "takes into account some of the correlation" because the spatial wave functions vanish when electrons come close together, so that the correlation energy difference $\Delta E_C(A - A^-)$ is rather small. For antiparallel spins the radial wave function of these two electrons is symmetric, and HF is then expected to be a poorer description, resulting in much larger $\Delta E_C(A - A^-)$ values. McKoy and Sinanoğlu [216, 217] have investigated theoretically the several contributions to these correlation energy difference trends in atoms and positive ions. They show [216] that the trends described above result from substantial changes in both the ns^2 and the $(ns^2 \rightarrow np)$ pair correlation energies upon addition of an np electron.

In addition to the ab initio calculations shown in table 3b, a number of other important contributions to this field have been made, such as the work by Schaefer et al. [82, 83, 94], Öksüz and Sinanoğlu [84, 85], Bagus et al. [86], Kancerivicius [73], LeDourneuf and Vo Ky Lan [89]. These calculations are mostly ab initio in nature, although Schaefer et al. [83] and Öksüz and Sinanoğlu [84, 85] added semiempirical corrections to their ab initio calculations to arrive at their final EA estimates. The approach of LeDourneuf and Vo Ky Lan [89] shows promise for obtaining accurate electron affinities in the future. Their multiconfiguration frozen core method may be described as a combination of variational MCHF procedures with polarized close-coupling ($e^- - A$) scattering calculations extended to bound states of A^-; it can be regarded as a generalization of the approach used by Norcross [66a] for the calculation of the alkali atom electron affinities.

2.4. Calculations of Electron Affinities for Higher Z Atoms

Clementi and co-workers have done a complete study of negative ions up to $Z = 29$ [44, 45, 50, 51]. The basis of their work is a calculation of accurate (restricted) Hartree-Fock energies of neutral atoms, positive and negative ions, coupled with estimates of the relativistic corrections E_R. By comparing known ionization potentials of atoms and positive ions, they

deduced the correlation energy E_C in the atoms and positive ions. They then determined electron affinities by estimating the correlation energy in the negative ion, since (apart from spin-orbit splittings)

$$EA(A) = [E_{HF}(A) - E_{HF}(A^-)] + [E_C(A) - E_C(A^-)$$

$$+ E_R(A) - E_R(A^-)]$$

$$= \Delta E_{HF}(A - A^-) + \Delta E_{C+R}(A - A^-) \qquad (5)$$

where ΔE_{HF} and ΔE_{C+R} refer to the first and second bracketed term, respectively, and all the quantities except $E_C(A^-)$ had been calculated or determined by comparison with accurate experimental numbers.

Two procedures were used to obtain $E_C(A^-)$. The first one, considered to be more reliable and applied to negative ions with $Z \leq 13$, involved a direct extrapolation of the correlation energy along an isoelectronic sequence. In the second procedure, the difference $\Delta E_{C+R}(A_Z - A_Z^-)$ was simply set equal to $\Delta E_{C+R}(A_{Z+1}^+ - A_{Z+1})$; for example, the quantity $\Delta E_{C+R}(Cl - Cl^-)$ was taken to be $\Delta E_{C+R}(Ar^+ - Ar)$.

As expected, the latter procedure was found to be less accurate for small Z, but has given remarkably good electron affinity estimates for the second row (except for Na). The results for the first method agree well with experiment except for O and Na. Moser and Nesbet [95] have very recently performed ab initio calculations of the electron affinities of the second row atoms. The technique is essentially the same as that employed for the first row [47, 48], and their results are in reasonable agreement with experiment.

Tables 4 and 5 summarize the results of various EA calculations for the first and second row atoms and provide a comparison with the best experimental values and with numbers obtained by *strictly* semiempirical methods to be duscussed in the next section.

One could have hoped that Clementi's results for the iron series $(K \rightarrow Cu)$ [51] would provide reliable estimates, but a comparison with the few experimental results available (table 6) shows that Clementi's numbers are too high by several hundred millielectron volts. It appears that the approximation

$$\Delta E_{C+R}(A_{Z+1}^+ - A_{Z+1}) = \Delta E_{C+R}(A_Z - A_Z^-), \qquad (6)$$

is not very good for $ns - ns^2$ transitions (with which we are mainly concerned here). It yields EA's [50, 51] for Li, Na, and K which are too high by 0.53, 0.36, and 0.41 eV, respectively.

The overestimate of EA(Li, Na, K) by use of the approximation eq (6) can be qualitatively understood from the trend in the correlation energy for isoelectronic atomic systems with one or two outer ns-electrons $(n = 2, 3, 4)$ around filled inner shells. The correlation energy associated with a single ns electron, due to interaction with the filled inner p- and s-shells, is small and varies little with Z on an absolute scale. The correlation

energy for the ns^2 system is mainly the pair-correlation energy, which increases noticeably with Z in the neighborhood of the neutral atom, before it eventually becomes constant for large Z. For the elements $Sc \rightarrow Cu$ this simple picture changes because of the strong interaction between the $3d$- and $4s$-shells; it is interesting that Clementi's results [51] for these atoms are high by similar amounts as for the alkali-atom EA's determined using eq (6), at least in those cases where comparison with experiments is possible (see table 6).

A model potential calculation on Cu^- was carried out by Schwarz [68] with the same technique which had yielded EA's for Li, Na, K, and Rb in excellent agreement with experiment. Schwarz determined $EA(Cu) = 0.7$ eV with an error "expected to not exceed a few tenths of an eV." Although the model potential method accounts for intershell correlation through the empirically adjusted effective potential, the deviation of Schwarz's result from experiment by 0.53 eV appears to indicate an improper representation of the $s-d$ intershell effects in Cu^-. Similarly, the pseudopotential calculations by Szasz and McGinn [65] have yielded rather poor results for Cu^- and Ag^- (too low by 0.45 eV), whereas they agreed satisfactorily with experiment for the alkali negative ions.

3. Semiempirical Methods: Isoelectronic Extrapolation, Horizontal Analysis

The atomic number Z, the number of electrons N in an atom or ion, and its degree of ionization q are connected by $Z = N + q$ (so that $q = 0$ for a neutral atom and $q = -1$ for a singly charged negative ion). Any two of these three quantities specify the atomic system under consideration. The various semiempirical methods for the comparison of different spectra correspond essentially to the choice of keeping either N fixed (isoelectronic extrapolation, IE), or q fixed (horizontal analysis, HA), or Z fixed (vertical analysis, VA). The procedures most frequently used are IE [96–98, 103, 105–113] and HA [99–102].

The various forms of isoelectronic extrapolations and horizontal analysis have been reviewed in some detail by Moiseiwitsch [26] and we refer the interested reader to this clear survey of the field. Part of the following discussion may repeat what is said there, but is included for completeness.

Isoelectronic extrapolation, in its most simple form for the extrapolation of electron affinities utilizes the expression [96, 109]

$$EA(Z_{-1}) = I(Z_{-1}) = 3I_0(Z_0) - 3I_1(Z_1) + I_2(Z_2), \qquad (7)$$

where I_0, I_1, and I_2 are the ionization potentials and Z_0, Z_1, and Z_2 are the atomic numbers of the neutral atom and the singly and doubly-charged positive ions of the isoelectronic sequence. This formula, originally suggested by Glockler [96], can be justified by perturbation theory and is found to give generally accurate results

TABLE 4. Comparison of calculated and recommended electron affinities (eV) for first row atoms

	Li	B	C	N	O	F
EA (Restricted HF) [45]	0.12	−0.27	0.55	−2.15	−0.54	1.36
Recommended EA	.620(7)	.28(1)	1.268(5)	−.07(8)	1.462(3)	3.399(3)
Recommended EA$_{SOC}$[a]	0.620(7)	0.28(1)	1.272(5)	−0.07(8)	1.465(3)	3.416(3)
Calculated EA's						
Clementi and McLean [44] HF + E_C extrapolation	0.58(5)	0.30(5)	1.17(6)	−0.27(11)	1.22(14)	3.37(8)
Schaefer et al. [83] CI + semiempirical correction		.19(10)	1.24(10)	−.21(10)	1.46(10)	3.45(10)
Öksüz and Sinanoğlu [84, 85] MET correlation calculation + semiempirical estimate			1.17	−.45	1.24	3.23
Weiss et al. [59, 80, 81] ab initio (symmetry-adapted pair-correlation) calculation	.62				1.47	3.47
Moser and Nesbet [47] ab initio (Bethe-Goldstone calc.; orbital excitation)		.22	1.29	−.12	1.43	3.37
Sasaki and Yoshimine [49] ab initio (CI)		.15	1.11	−.52	1.13	3.12
Sasaki and Yoshimine [49] best estimate based on CI-calculation		.24	1.23	−.19	1.47	3.48
Kancerivicius [73] ab initio MCHF	.62	.03	1.07	−.99	0.79	2.87
Glockler [96] quadratic IE	0.42	−0.10	0.92	−0.56	1.01	3.04
Edlén [97] IE	.82[b]	.33	1.24	.05	1.47	3.50
Kaufman [98] IE	.64	.39	1.32	−.31	1.26	3.24
Ginsberg and Miller [99] HA		.34	1.37	−.32	1.38	[3.40]
Edie and Rohrlich [100] HA		.33	1.38	−.15	[1.46]	3.47
Crossley [101] HA	.59	.16	1.33	−.32	1.39	[3.45]
Zollweg [102] HA		.18	1.29	−.21	[1.46]	3.50
Hunt and Moiseiwitsch [103] model potential radius IE	.69	.05	1.15	<0	1.39	3.69

[a] Since none of these calculations included spin-orbit coupling, this quantity, the recommended EA, modified to correspond to the energy difference between term centers-of-gravity, is the one most relevant for comparison with these calculations.

[b] More recently, Edlén obtained EA(Li)=0.64 eV by use of a somewhat different formula [103].

TABLE 5. Comparison of calculated and recommended electron affinities (eV) for second row atoms

	Na	Al	Si	P	S	Cl
Restricted HF calculation [50]	−0.12	0.02	0.96	−0.54	0.91	2.58
Recommended EA	.546(5)	.46(3)	1.385(5)	.743(10)	2.0772(5)	3.615(4)
Recommended EA$_{SOC}$ [a]	0.546(5)	0.46(3)	1.404(5)	0.731(10)	2.0813(5)	3.651(4)
Author and Method						
Clementi et al. [50] HF + E$_C$ extrapolation	0.78(6)	0.49(14)				
Clementi et al. [50] HF + E$_{C+R}$ estimate	.91	.52	1.39	0.78	2.12	3.56
Moser and Nesbet [95] Bethe-Goldstone orbital excitations, one and two particle terms		.49	1.52	.74	2.18	3.79
Glockler [96] quadratic IE	−0.05	0.03	1.07	0.38	1.79	3.39
Edlén [97] IE	.47	.52	1.46	.77	2.15	3.70
Ginsberg and Miller [99] HA (corrected)		.22	1.42	.54	2.03	[3.61]
Edie and Rohrlich [100] HA (corrected)		.20	1.30	.64	2.00	[3.61]
Crossley [101] HA	.22	.27	1.40	.62	2.03	[3.61]
Zollweg [102] HA		.20	1.36	.71	2.04	[3.62]
Hunt and Moiseiwitsch [103] model potential radius extrapolation	.66	.56	1.41	.74	1.96	3.68

[a] Since none of these calculations included spin-orbit coupling, this quantity, the recommended EA modified to correspond to the energy difference between term centers-of-gravity, is the one most relevant for comparison with these calculations.

(~ 0.1 eV) when used to determine ionization potentials of atoms and positive ions. Its use for obtaining EA's does not lead to accurate results (see tables 4, 5). Therefore modifications to eq (7) have been suggested and used by Johnson and Rohrlich [106], Edlén [97] Baughan [108] Kaufman [98], and Scherr et al. [112] for EA extrapolations; these corrections basically amount to the addition of one or two further terms from the perturbation series expansion for the ionization potential as a function of Z. Edlén's [97] correction term Q does not contain any new parameters, but is expressed in terms of I_0, I_1, I_2 and n, where n represents the principal quantum number of the electron added to form the negative ion:

$$Q = \frac{3(I_0 - 2I_1 + I_2 - 2R/n^2)(-I_0 + 2I_1 - I_3 + 6R/n^2)}{I_0 - 4I_1 + 3I_2 - 12R/n^2},$$
(8)

$$EA = 3(I_0 - I_1) + I_2 + Q,$$

where $R =$ Rydberg constant.

Edlén's eq (8) [97] yields a considerable improvement over the use of the earlier simple expression in the iso-electronic extrapolation of electron affinities for the first two rows of the periodic table (see tables 4 and 5), and gives good agreement with the experimental data in most cases. In spite of the apparent success of Edlén's formula, it has been pointed out, for instance by Edie and Rohrlich [100], and discussed further by Crossley [101], that there is no obvious theoretical explanation for the success of Edlén's formula. The Edlén Q cannot actually be regarded as a correction in the sense that it represents higher members in a perturbation series expansion. The magnitude of Q is not necessarily small compared with the estimate resulting from eq (7) and, furthermore, addition of the next higher members in the series beyond Q may lead to results which are in poorer agreement with experiment. Kaufman [98] has also discussed these points in some detail and arrived

at somewhat different conclusions. She points out that the validity of the Z-dependent expansion for the calculation of electron affinities provides criteria for the optimal determination of the expansion coefficients, and also indicates that relativistic terms should be included in the expansion.

The most recent review on isoelectronic extrapolation by Edlén [104] reflects the status of these methods as applied to atoms and ions containing up to ten electrons. Only little attention, however, is given to isoelectronic extrapolation of electron affinities; the application of an expansion, found to fit four-electron ionization potentials, to the EA(Li) yielded 0.64 eV [104], in good agreement with experiment. We have applied Edlén's formula [104] (without relativistic terms) for nine- and ten-electron systems to O^- and F^-, and find after the appropriate corrections for spin-orbit splittings: EA(O) = 1.30 eV and EA(F) = 3.26 eV. The deviation from the experimental numbers may, at least in part, be due to the omission of relativistic corrections.

Horizontal analysis [99–102] is the other frequently used method for estimating electron affinities. The HA approach is based on the regular behavior of ionization potentials for species with the same degree of ionization q. Specifically, it is found that within each p-shell the "generalized" ionization potential, i.e. the energy difference between the respective ground configuration centers, as a function of Z (q fixed), is very nearly a linear function of Z [100, 102, 105]. The slopes of such lines are very nearly linear functions of q and one extrapolates the slope to the negative ion case, $q = -1$. The energy levels of the different negative ion terms of the same ground configuration can then be estimated by means of isoelectronic extrapolation, eq (7). It has been recognized that this simple quadratic extrapolation formula yields much better results for these energy *differences* than it does for electron affinities directly. Improved estimates of the term splittings were obtained by Moiseiwitsch [26] using eq (8).

The absolute values of the electron affinities derived by horizontal analysis have been commonly adjusted to fit one benchmark ion in a horizontal series. Typical choices have been oxygen or fluorine for the first row and chlorine for the second row. In tables 4 and 5, the corresponding benchmark EA is listed in brackets. The results of some representative extrapolation studies (IE and HA) are listed and compared to both ab initio calculations and experimental data in tables 4 and 5, for the atoms of the first and second row of the periodic table. All semiempirical results agree rather well with experiment.

Zollweg [102] has also estimated electron affinities for all the main group elements of the third, fourth and fifth rows by horizontal analysis of the type described above. His results agree to within 0.2 eV or better with the available accurate experimental determinations.

In view of the limited experimental work done on the negative ions of the long series of the periodic table (elements K to Cu, Rb to Ag, Cs to Au), and the very limited theoretical work on these ions [51, 65, 68] extrapolation techniques are a primary source of information for estimates of the EA of these atoms. For this reason it is important to elaborate further upon the Zollweg analysis [102] of the three long series.

The essential point in the Zollweg analysis is that the energy difference between the two configurations $d^k s^2$ and $d^k s$ ($k = 0, \ldots, 10$) of the two adjacent degrees of ionization increases nearly linearly with k for a given q. It is probable that the ground state configuration of negative ions in the three long series is $d^k s^2$ [51, 102, 107, 110]. One can therefore estimate the EA's of these atoms if those for K, Rb, Cs on the one side and those for the Cu, Ag, and Au on the other side are known, because then the slopes of the straight lines representing the $d^k s^2 \rightarrow d^k s$ energy differences are known. The numbers used for those benchmark EA's by Zollweg [102] are now superseded by accurate photodetachment results [9, 10, 14]. In table 6 is presented a recalculation of the EA's for the atoms in the long series using Zollweg's method including half of the correction adopted by Zollweg [102] to account for small deviations of the $d^k s^2 \rightarrow d^k s$ energy differences from the straight line behavior observed for $q = 0$. Also shown in table 6 are values obtained by Charkin and Dyatkina [110] for the first two long series. These authors use the Glockler method [96] plus a constant correction chosen to give agreement with the alkali-atom affinity (in the second long series we subtract 0.11 eV from their estimates since they had normalized to EA(Rb) = 0.6 eV, which has since been determined to be 0.4860 eV). Implicit in their results — as in Zollweg's — is the assumption that the negative ion ground state has $d^k s^2$ configuration.

The accuracy of these predictions for the electron affinities of the elements of the three long series is hard to assess; however, we tend to prefer those obtained by the horizontal analysis for two reasons:

(a) They are fixed to solidly established numbers at *both* ends of the series and they make use of a regularity in an energy difference which has been established for both $q = 0$ and 1.

(b) The Glockler method, although easy to use, is known to give rather poor results for EA's of other elements; moreover the use of a *constant* additive correction to the actually extrapolated EA's is a rather arbitrary procedure, which has no theoretical basis.

It may be somewhat surprising that the two sets of numbers are found to agree within 0.3 eV or better in all cases except Y, Zr, and Pd. The largest difference observed is that for Pd, amounting to 0.9 eV. We believe that the smaller electron affinity of Pd (0.4 eV derived with HA), is more reasonable since the ground state of Pd is $4d^{10}$, with the $4d^9 5s$ state lying about 0.8 eV higher. If the assumption about the $4d^9 5s^2$ character of the negative ion ground state is correct, one would judge that an EA so reevaluated with Zollweg's method should

TABLE 6. Electron affinities[a] of the elements in the long series

Author & Method	K	Ca	Sc	Ti	V	Cr	Mn	Fe	Co	Ni	Cu
Clementi [51] HF + E_{C+R} est.	0.92(5)		-0.14(10)	0.40(20)	0.94(25)	0.98(35)	-1.07(20)	0.58(20)	0.94(15)	1.28(20)	1.80(10)
Charkin and Dyatkina QIE with +0.5 correction [102]	[.50]	-1.62	-.39	.15	.65	.85	-1.19	.11	.72	1.10	1.35
Present HA[e]	[.50]	-1.90	-.75	-.11	.46	.73	-1.28	.09	.62	1.13	[1.23]
Experiment	.5012(5)[b]					.66(5)[c]				1.15(10)[c]	1.226(10)[b]
Recommended	.5012(5)	<0	<0	.2(2)	.5(2)	.66(5)	<0	.25(20)	.7(2)	1.15(10)	1.226(10)

Author & Method	Rb	Sr	Y	Zr	Nb	Mo	Tc	Ru	Rh	Pd	Ag
Charkin and Dyatkina QIE with +0.54 eV correction [110]	[0.49]	-0.61	0.19	0.93	1.21	1.17	0.85	1.33	1.23	1.29	1.37
Present HA[e]	[.49]	-1.50	-.47	.3	.90	.88	.61	1.05	1.13	.40	[1.30]
Experiment	.4860(5)[b]				1.0(4)[d]	1.0(2)[d]					1.303(7)[b]
Recommended	.4860(5)	<0	.0(3)	.5(3)	1.0(3)	1.0(2)	.7(3)	1.1(3)	1.2(3)	.6(3)	1.303(7)

Author & Method	Cs	Ba	La	Hf	Ta	W	Re	Os	Ir	Pt	Au
Present HA[e]	[0.47]	-0.46	0.51	-0.73	0	1.02	0.12	1.12	1.59	2.13	[2.31]
Experiment	$.4715^{b}\binom{5}{20}$				0.8(3)[d]	.5(3)[d]	.15(10)[d]			2.218(2)[b]	2.3086(7)[b]
Recommended	$.4715\binom{5}{20}$	<0	.5(3)	<0	.6(4)	.6(4)	.15(10)	1.1(3)	1.6(2)	2.218(2)	2.3086(7)

[a] $d^k s^2$ configuration in the negative ion state is assumed in calculation of EA and for recommended values.   [e] Using the method of Zollweg [102]. See text.
[b] Lineberger, et al. [9, 10, 14].   [c] Feldmann, et al. [20, 114, 115].   [d] Scheer [116–118].

normally be correct within about 0.2 to 0.3 eV. For the first long series (K → Cu) in table 6, we have also listed Clementi's results, which have already been discussed in section 2.4. They are consistently too high by a few tenths of an electron volt.

Two atomic radius extrapolation techniques should be mentioned briefly: the vertical-radius analysis by Politzer [119] and the model potential radius extrapolation of Hunt and Moiseiwitsch [103]. The Politzer approach correlates the difference between the ionization potential and the electron affinity of atoms with their atomic radius, $\langle r \rangle$. A plot of log (IP–EA) against $\log(1/\langle r \rangle)$ is found to give a straight line for ions within the same (vertical) family. The EA's for the elements in groups 3A to 6A (third to fifth row) were extrapolated by using experimentally determined EA's (or those calculated by Clementi et al.) for the corresponding elements in the first two rows, known IP's and known $\langle r \rangle$ values from Hartree-Fock calculations. The agreement with experiment is rather poorer than the Zollweg analysis in most cases. One obvious disadvantage of this method is the insensitivity to EA. Clearly, the quantity (IP – EA) is not much different from IP; in order to obtain a reliable EA the logarithm of (IP – EA) has to be very well determined.

The other extrapolation technique, adopted by Hunt and Moiseiwitsch [103], used a model-potential radius extrapolation both for the determination of EA's and for the location of shape resonances (EA < 0) in electron-atom scattering. The cut-off radius separating the inner and outer regions of a simple model potential was derived for the isoelectronic neutral atom, singly and doubly charged ion systems, using known ionization potentials; with this knowledge the radius for the model potential of the negative member of the isoelectronic sequence was obtained by quadratic extrapolation. The EA's obtained are in fair agreement with the experimental results, especially for the second row atoms (see tables 4 and 5).

In summary, it appears that the "best" semiempirical extrapolations of electron affinities have yielded estimates of accuracy comparable to the best currently available ab initio calculations (except H and the alkali atoms) or Hartree-Fock calculations augmented by correlation energy estimates. Whether the predictions obtained from horizontal analysis for the long series elements can indeed be viewed as a reliable guideline within the estimated 0.2 eV to 0.3 eV uncertainty remains to be seen.

In addition to the semiempirical methods discussed above, still other approaches have been taken to derive electron affinities from various experimental data in a more or less indirect way, e.g. *lattice* calculations [23, 26], or conclusions from *potential curves* [120, 121]. Since we are concerned here with the properties of free negative ions, we shall not include a discussion of atomic negative ions in solutions or solids. In most cases the validity of these approximate methods can now be tested

by comparison with known electron affinities; atomic binding energy information is normally not obtained with the accuracy of other methods discussed in this review.

## 4. Experimental Methods for Measurement of Binding Energies in Atomic Negative Ions

The primary purpose of this section is to provide a brief description of the major experimental methods that have been utilized to provide information on binding energies in atomic negative ions. Since, of the major experimental methods, only the laser photo-detachment experiments have not been extensively discussed in the review literature, a more complete review of these techniques is presented. For those other methods that have produced binding energy data which have been incorporated into the set of "recommended" affinities (table 10), a more limited description is given, but an attempt is made to point out the major assumptions and theoretical formalisms required to extract binding energy information from the raw experimental data. Where possible, we give our assessment of the accuracy possible with each method under favorable conditions. Several other methods (e.g., ion cyclotron resonance spectrometry and electron dissociative attachment) have made major contributions to the understanding of negative ions, but no data using these methods appear in table 10; these techniques are briefly mentioned for completeness. The literature cited in this section will include the basic papers, which provide descriptions of apparatus and techniques, the analysis of the data, representative measurements; and a sufficiently large sample of recent publications to provide entry into all of the early literature.

For the purposes of this discussion, we have subdivided the experimental methods into direct methods, indirect methods, and qualitative methods. By direct methods we mean those experimental techniques that provide numerical determinations of binding energies with recourse only to such basic concepts as conservation of energy and conservation of momentum. Included in this category are (1) photodetachment under collision-free conditions, (2) plasma absorption and emission studies, and (3) photodissociative ion pair formation. While it seems possible that, at the level of a few milli-electron volts, a substantial amount of plasma physics may have to be invoked in order to understand the threshold behavior in the plasma experiments, it appears certain that at the 10 meV level the determinations are essentially direct. Included among the indirect methods are surface ionization, ionization by strong electric fields, dissociative electron attachment, and charge exchange. The reasons for calling these methods indirect, on a 10 meV scale, will be made clear in the following sections. The qualitative determinations are essentially those that report only the existence of a negative ion. They will not be discussed in this paper,

even though such data may be the only information available in a few cases.

4.1. Photodetachment under Collision-Free Conditions

It has long been recognized that, in principle, the most unambiguous and accurate method for determination of atomic electron affinities is to study the photon energy dependence of the photodetachment process,

$$h\nu + A^- \rightarrow A + e,$$
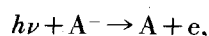
under conditions where A^- is in a field-free region and suffers no collisions for times the order of the length of time the negative ion interacts with the photons. Under these conditions, a determination of EA(A) consists essentially of a determination of the long wavelength threshold for photodetachment. (Fine-structure considerations will be discussed later in this section.) In this case, the only physics one is invoking is conservation of energy and the only quantity that has to be measured absolutely in order to determine an electron affinity is the wavelength of the light corresponding to the threshold. Given a means of detecting one of the photodetachment reaction products with adequate sensitivity, one can measure an electron affinity directly and unambiguously with an accuracy of the order of the bandwidth of the photon source.

Photodetachment utilizing crossed ion and photon beams with conventional light sources was first employed in a series of very elegant and beautiful experiments by Branscomb and his colleagues [122–128]. This approach will be discussed in more detail in the following section. Since the advent of tunable dye lasers as a photon source for photodetachment experiments, the accuracy with which one can determine electron affinities experimentally has been greatly increased, and the nature of the uncertainties in electron affinity determinations has changed qualitatively. For this reason the dye laser photodetachment measurements [7–9, 14] will be discussed separately in the next section.

The recently developed ion trapping devices provide an alternative to crossed beams for studying ion-photon interactions under collision-free conditions. While this approach has been utilized to date only for studies of molecular negative ions (where it is most advantageous), one could accurately determine atomic affinities in such a system. Trapping schemes will accordingly be discussed in the third section.

Another variant of the crossed beam photodetachment technique is to study the photodetachment process in a crossed ion beam-fixed frequency laser beam geometry, under conditions in which the photon energy is significantly greater than the electron affinity of the atom under study, and to measure the kinetic energy of the ejected electron [2–6, 10, 14, 15]. While electron kinetic energies cannot be measured as accurately as photon

energies, and hence the EA determinations are not as precise as possible optically, the resulting electron affinities are direct and unambiguous; with care one can obtain electron affinities accurate to the few milli-electron volt level. This laser photoelectron spectrometry method (LPES), developed by Hall and colleagues [2–6], has only become possible with the advent of suitable laser light sources. It has provided a wealth of information on atomic negative ions in recent years [2, 10, 14, 15, 19, 129, 130] and will be discussed in some detail in the last section.

4.1.a. Crossed Photon-Ion Beam Using Conventional Light Sources

The basic idea is to intersect a moderately energetic (a few kiloelectron volts) mass-analyzed negative ion beam with the spectrally resolved light from an intense light source, such as a high-pressure xenon arc lamp. One then detects either the photodetached electrons or the neutral atoms resulting from the photodetachment process, as a function of the photon energy. The first such apparatus was built by Branscomb and colleagues in the 1950's [122, 123]; variants of the same apparatus have been utilized by Steiner [131, 132] and by Feldmann [133, 134] to determine atomic electron affinities. The detailed signal-to-noise considerations which go into measurements of this type have been discussed thoroughly in several excellent reviews [25, 30, 33], and only a brief summary will be presented here.

Since, in all of these experiments, the initial photon source consists of a continuously operating black body-type source, there is a rather definite limit to the maximum brightness per unit wavelength interval that can be obtained. The dominant source of background in these experiments consists of neutrals or electrons produced from collisional destruction of the negative ions on the residual background gas,

$$A^- + B \rightarrow A + B + e. \tag{9}$$
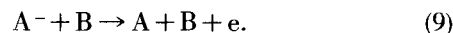
Even if one chops the photon and ion beams, and uses phase sensitive detection to differentiate between photodetachment reactions and background gas reactions, the detection of the photodetachment products becomes very difficult when the ratio of photodetachment products to collisional stripping products becomes less than 10^{-4}. This consideration essentially sets the minimum photon energy bandwidth that can be employed in such measurements, for a given background gas pressure and stripping cross section [25, 30, 33].

All such measurements to date have been performed in vacuum systems with base pressures the order of 10^{-8} Torr; at this pressure the highest photon energy resolution obtained to date in a favorable case was $\Delta\lambda = 18$ Å at 4000 Å (energy spread 15 meV FWHM) in an experiment on the first I^- threshold [128]. More typically, bandwidths between 50 and 200 Å could be utilized. By deconvolution of the observed cross section

with the known light intensity profile, Branscomb and colleagues have, in the most favorable cases (sharp thresholds), determined electron affinities to an accuracy of a few millielectron volts [125, 128]. Such determinations become much less precise if the required photon energy bandwidth is so broad as to obscure transitions between fine-structure levels of the negative ion and the neutral atom [132].

With the significant advances in vacuum technology that have occurred since Branscomb's original apparatus was built, it is perfectly possible to build a crossed beam photodetachment apparatus using conventional light sources in which the pressure in the interaction region is 10^{-10} Torr or less; under these conditions the signal-to-noise criteria discussed above would permit a photon energy resolution of order 1 Å, and would make this photodetachment technique competitive in resolution with the dye laser photodetachment methods. It seems somewhat surprising that this approach has not yet been attempted.

In the past two years, a large number of atomic negative ion photodetachment cross sections have been measured by Feldmann and colleagues at Hamburg and Heidelberg [20, 114] using a Branscomb-type apparatus. They have made a major improvement in the apparatus in that they are utilizing a high-intensity, versatile negative ion source, developed by Heinicke [16, 17], which is capable of producing high-intensity negative ion beams (30 to 1000 nA) of most elements of the periodic table [16]. The intensity of the light source employed is similar to that utilized by Branscomb, and the pressures in the collision region are comparable, so that the resolution they can obtain in the photodetachment measurement is the order of 50 to 200 Å. The negative ions they have studied have frequently exhibited excited states and complicated, unresolved fine structure, which have limited the accuracy of their electron affinity determinations to about 50 meV in many cases. Since their light source contains substantially more complicated line structure than that utilized by Branscomb, Feldmann and his colleagues have not attempted to deconvolve any of their data with the finite bandwidth of the light source. In the most favorable cases in which fine structure is absent (the alkalis) the accuracy of these measurements is about 20 meV. Light source limitations have precluded measurement of electron affinities less than approximately 0.5 eV.

By utilizing the experimentally determined 0^- absolute photodetachment cross section as a reference, these authors have measured absolute photodetachment cross sections for about a dozen atomic negative ions in the photon energy range 0.5 to 3.0 eV [79, 115]. A number of these determinations show very interesting structures and evidence for excited states of negative ions. In many cases the complexity of the structures, together with unresolved thresholds, have, however, hindered attainment of accurate electron affinities. Clearly, higher resolution in such experiments is desirable; the

tunable laser techniques described in the next section provide one such answer.

4.1.b. Crossed Photon-Ion Beam Using Tunable Dye Lasers

Utilizing the light sources described in the preceding section, together with a fast monochromator, the amount of light which may be focused onto an ion beam is of the order 10^{-3} W/Å. The discovery of laser emission from excited organic dye molecules in 1966 by Sorokin and Lankard [135] and, independently, by Schäfer, Schmidt, and Volze [136] has qualitatively changed the character of light sources available for photodetachment. Relatively simple flashlamp-pumped dye lasers are capable of producing intense, narrow line width (1 Å or less) radiation which can at present be continuously tuned across the spectral region 4400 to 7500 Å. Typical outputs of such dye lasers are energies of approximately 1 mJ in a pulse of duration 0.3 μs, resulting in peak powers substantially greater than 10^3 W/Å! Thus the dye laser provides an increase of at least 6 orders of magnitude in the signal-to-noise ratio, and indicates that, during the time the laser pulse is on, the ratio of photodetached neutrals to stripped neutrals can be greater than 10^2. Details of the operation of dye lasers, their capabilities and the applications for which they are being utilized are discussed in reviews by Schäfer [60], Demtröder [137], Lange, Luther, and Steudel [138], and Moore [139].

The first application of dye lasers to photodetachment studies was an investigation of the threshold photodetachment of the sulphur negative ion by Lineberger and Woodward in 1970 [7]; fairly detailed descriptions of the apparatus and technique have been published [8], to which the reader is referred for further details. In this apparatus, shown in figure 1, a flashlamp-pumped tunable dye laser is substituted for the light source in a Branscomb-type apparatus. A several kiloelectron volt mass-analyzed negative ion beam is intersected with the photon beam from a tunable dye laser, and a cross section for production of neutral atoms is measured as a function of the laser wavelength. The negative ions are formed in one of several types of discharge sources,
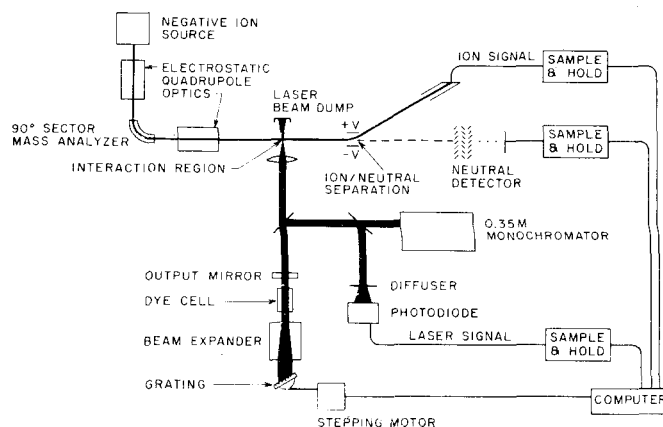

FIGURE 1. Schematic diagram of the tunable laser photodetachment apparatus ([8], with permission).

accelerated, mass analyzed, and focused onto a window-less electron multiplier located 20 cm beyond the laser beam-ion beam intersection. After passing through the interaction region, but before reaching the multiplier, the ions are electrostatically deflected into a Faraday cup, so that only neutral atoms produced by charge stripping on the background gas and by laser photodetachment, reach the neutral detector. In order to take advantage of the brightness of the pulsed laser, time-gated detection is used for the various ion, neutral and photon signals. As a result of the large number of neutrals reaching the multiplier in a short time interval, this detector is operated in a linear, charge-amplifying mode rather than as a particle counter.

The 1 Å wavelength resolution is adequate in most cases to resolve the various fine-structure transition thresholds necessary for an unambiguous determination of an electron affinity. For example, in studies of photodetachment of Se$^-$ p^5 $^2P_{1/2,3/2}$ one expects to see six thresholds corresponding to photodetachment from each of the negative ion fine-structure levels to the $^3P_{2,1,0}$ levels of Se. Moreover, if such thresholds can be seen, the fact that the neutral atom fine-structure intervals are well known spectroscopically can be used to identify unambiguously which threshold corresponds to which transition. Figure 2 shows a broad range of the Se$^-$ photodetachment cross section measured using a tunable dye laser as the light source in a crossed beam apparatus [8]. Detailed threshold studies show that each of the indicated fine-structure intervals in Se are within ±2 cm^{-1} of the known Se spectroscopic splittings. Thus, the identification of the transition corresponding to the electron affinity ($^2P_{3/2} \rightarrow ^3P_2$) is readily made and the remaining task is to measure the wavelength corresponding to this threshold.

The 1 Å resolution permits a test of the validity of the leading term of the appropriate photodetachment threshold law in the process of determining the electron affinity [7–9]. Thus, figure 3 shows the square of the
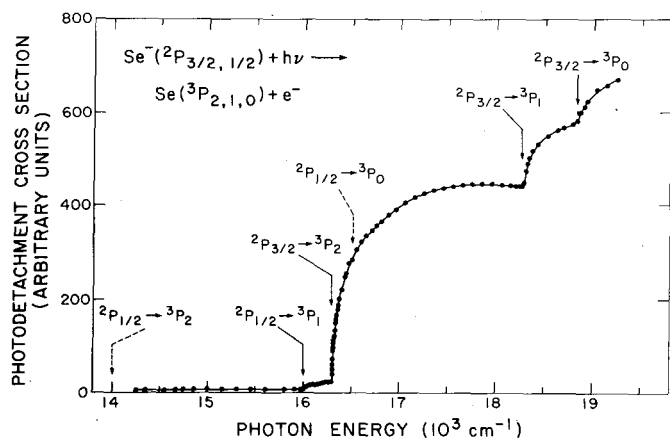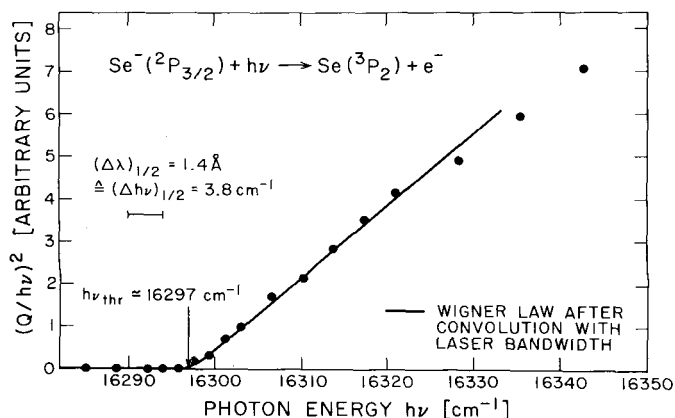

FIGURE 3. Se$^-$ photodetachment data near the $^2P_{3/2}$–$^3P_2$ onset. The cross section below the threshold has been subtracted from the observed cross section to obtain these data. The solid curve represents the Wigner threshold law convolved with the laser line width, and indicates that the threshold energy is determined to ±2 cm^{-1} ([8], with permission).

Se$^-$ $^2P_{3/2} \rightarrow ^3P_2$ cross section plotted as a function of photon energy in the region near threshold [8]. For this case, detachment of a bound p-electron, the Wigner threshold law [140] predicts $\sigma \propto k$, a straight line on such a plot. Here k is the magnitude of the momentum of the detached electron. It can readily be seen that there are noticeable departures from the Wigner threshold law only 5 meV above the threshold. If one convolves the now-tested threshold law with the measured line width of the laser and shifts such a curve so as to obtain a best fit to the experimental data, one obtains the solid line shown in figure 3. Such a fit can be made to an accuracy of ±2 cm^{-1}, corresponding to an uncertainty in the electron affinity determination of ±0.0003 eV.

The major sources of error in such a determination are as follows:

(1) identification of the appropriate threshold,
(2) finite line width of the laser,
(3) wavelength measurement,
(4) Doppler shifts and broadening of the threshold due to divergence of the ion and laser beams, and imprecise determination of the angle at which the ion and laser beams intersect.

If enough thresholds are seen, then the proper assignment of the EA transition is unique. The line width of the laser employed in the above studies was 1.4 Å, corresponding to a photon energy uncertainty of 0.5 meV. There exist techniques [60, 138, 139] for reducing the laser line width to the milliangstrom level or lower, thus reducing possible error from this source to the submicroelectron volt level. In the study reported above the uncertainty in the wavelength determination was ±0.2 Å. Given a sufficiently narrow laser line width, there now exist standard, albeit difficult, methods for measuring the wavelengths to accuracies of the order 1 part in 10^8. Thus, if desired, this source of error could be reduced to the submicroelectron volt level, a level where one has to think about the effects of hyperfine structure!

FIGURE 2. Se$^-$ photodetachment cross section in the energy range 14,000 to 19,000 cm^{-1}. The individual fine-structure transition thresholds are indicated on the figure ([8], with permission).

The laser frequency, in wave numbers, determined in the laboratory frame, must be transformed into the moving frame of the negative ions. In the experimental arrangement cited above, the angle θ was $(90 \pm 2)^\circ$ which introduced a possible Doppler shift of 0.1 cm^{-1} (12 μeV) at the Se$^-$ velocity employed. If the ion and laser beams are not perfectly collimated, the Doppler effect also broadens the apparent line width, and hence the threshold. The ion beam divergence in the above case was limited by 4 mm apertures at the entrance and exit of the interaction region, corresponding to a maximum divergence half angle of approximately 1.2°. The lens that focuses the laser into the interaction region allows a maximum divergence of the laser beam of approximately 0.5°. The total divergence of the beams thus has an upper limit of the same order as the uncertainty in θ, resulting in another 0.1 cm^{-1}. The Doppler shift is also sensitive to the ion velocity distribution, although this introduces a negligible error in the present experiment. The ion energy can be expected to vary by, at most, half of the arc voltage in the ion source, which results in a 1 percent variation in the ion velocities and a maximum change of 0.001 cm^{-1} in the Doppler broadening.

The principal conclusion of this discussion is that, if the thresholds are properly identified, then the dye laser photodetachment technique can provide an unambiguous determination of an electron affinity with an accuracy of a few tenths of a millielectron volt. It also seems clear that, if one were willing to work hard enough the inherent resolution limitations present no fundamental restrictions on the accuracy of an electron affinity determination, at least to the level of a few microelectron volts.

While it might appear from the above discussion that the crossed ion beam-tunable laser beam approach provides the ultimate solution to all problems concerning binding energies in negative ions, such is certainly not intended to be the case. While it seems true that, if the criteria stated above are met, the tunable laser photodetachment results will be unambiguous and more accurate than those attainable with any other experimental technique proposed to date, there are a number of difficulties associated with these measurements. They include the following:

(1) limited wavelength regions accessible with current laser systems;

(2) complicated structure appearing near the threshold, requiring a substantial theoretical formalism to determine the actual threshold;

(3) interpretation of molecular photodetachment data where individual thresholds are not resolved;

(4) absolute cross section measurements.

At present the wavelength region accessible to the fundamental frequency output of tunable organic dye lasers is from 3400 to 7500 Å, with very low output powers available in the wavelength region 3800 to 4300 Å. At substantially lower (but still usable) outputs,

frequency doubling extends the usable range to about 2300 Å. It appears that developing organic dye technology will increase the long wavelength limit to approximately 1 μm, but even longer wavelength outputs are unlikely because of absorption and decomposition problems in dye molecules. A substantial fraction of the atoms have electron affinities corresponding to photodetachment thresholds at wavelengths longer than 1 μm, and hence it is likely that their photodetachment thresholds will never be observed using tunable organic dye lasers. Other tunable light sources, such as the optical parametric oscillator, could fill this long wavelength gap, but at present they involve a substantial investment in time and money. The rapidly evolving nonlinear mixing techniques [141–143] may greatly increase the spectral range available at both long and short wavelengths, but the presently available output powers are marginal for photodetachment experiments.

The fact that one may be unable to see the photodetachment threshold leads naturally to an attempt to measure an electron affinity by observing a threshold for photodetachment into an excited state of the neutral atom, thereby shifting the threshold wavelength to shorter wavelengths, while still maintaining the ability to determine an electron affinity. Such studies have been undertaken for the alkali negative ions, in which photodetachment was investigated [14] at wavelengths corresponding to leaving the alkali atom in its first excited ($^2P_{1/2, 3/2}$) states. In these studies the photodetachment cross section behavior near the excited state threshold was frequently much more complicated than had been expected from a simple theoretical picture, because there are doubly excited states of the negative ion lying just below the parent excited neutral state. For example, figure 4 shows the highest resolution photodetachment data obtained to date [144], with resolution approxi-
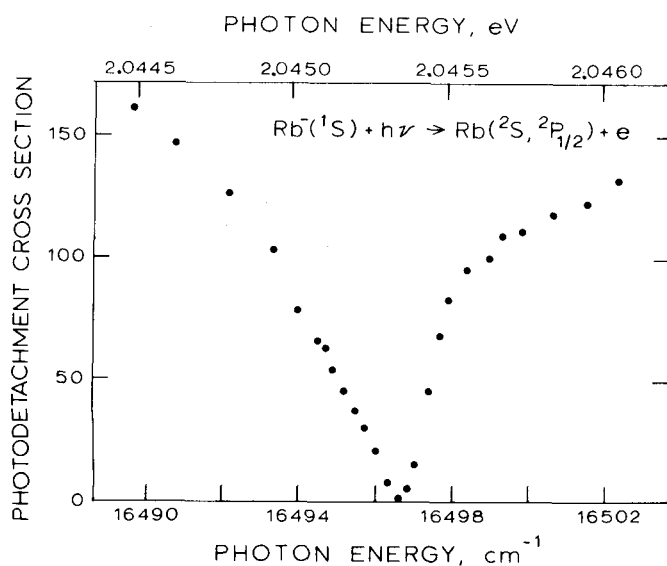

FIGURE 4. Rb$^-$ photodetachment cross section at the resonance which overlaps the Rb (5^{2}P$_{1/2}$) channel opening. These data represent the highest resolution photodetachment data obtained to date ([144], with permission).

mately 20 times greater than that employed in the Se⁻ studies. This figure shows the Rb⁻ photodetachment cross section in the photon energy region corresponding to the opening of the Rb $^2P_{1/2}$ exit channel. Through a somewhat involved argument, the photodetachment threshold for this state was determined to be the apparent discontinuity in the photodetachment cross section near 16,500 cm⁻¹. The prominent drop of the total cross section to zero is a result of a Rb⁻ autoionizing state lying very close to Rb $^2P_{1/2}$. It is clear that this discontinuity is not the dominant feature in this rather narrow wavelength region, and, as a result, the uncertainty which had to be assigned to this electron affinity determination is in fact slightly larger than that assigned in the Se⁻ case, which had 20 times poorer resolution.

In studies of photodetachment of molecular negative ions using tunable lasers, it is in general not possible to resolve individual rotational transitions, and the interpretation of the photodetachment cross sections in terms of a precise electron affinity is exceedingly difficult. While such studies have proven successful for small negative ions, such as OH⁻ [12], and moderately successful for more complex negative ions, such as NO₂⁻ [21], it is clear that there are more desirable and accurate methods available for determining molecular electron affinities in general. In addition, all of the crossed beam photodetachment experiments to date have utilized a negative ion source which produced negative ions at a large (approximately 1500 K) and ill-defined temperature. While the hot source is very useful in populating excited states of negative ions for study, it adds immensely to the complexity of the molecular negative ion photodetachment spectra, and cooler ion sources would be extremely desirable for molecular negative ion photodetachment studies.

All negative ion photodetachment studies have difficulty in the determination of *accurate* absolute photodetachment cross sections. This subject has been discussed at length in several reviews [25, 33, 30], and the tunable laser approach does not significantly change the problems encountered, or the accuracy with which absolute cross-section determinations can be made. Since such absolute cross-section determinations do not enter into the *direct* determinations of binding energies in atomic negative ions, the subject will not be discussed further.

The last point to be made is that any single determination requires a substantial experimental effort and investment of time. Since, in order to make any measurement at all, one must see most of the expected thresholds (or show the nonexistence of unexpected thresholds in the spectral region around the observed threshold), it is necessary to carefully study the photodetachment cross section over a rather wide wavelength region, and to measure a cross section with sufficient accuracy that one is convinced the threshold energy differences observed correspond to the appropriate neutral. Thus,

in effect, if one makes any measurement at all using this approach, one has probably made a measurement accurate to the millielectron volt level.

4.1.c. Photodetachment of Trapped Ions

Studies of the interactions of photons with ions stored in electromagnetic traps provides an alternative to the crossed beam technique for studies of photon processes under collision-free conditions.

Brauman and coworkers [145–151] have utilized an ion cyclotron resonance spectrometer to study the photodestruction of trapped negative ions. The concentration of a particular negative ion species is obtained by monitoring the radio frequency power absorbed from a marginal oscillator tuned to the cyclotron resonance frequency of that ion. Both conventional light sources and laser sources have been successfully utilized with the ion cyclotron resonance photodetachment apparatus. Perhaps the greatest advantage of this approach is that the trapped ions can be allowed to cool to a thermal distribution prior to irradiation and, largely as a result of this unique feature, all studies to date have been on molecular ions. Since the ion cyclotron resonance technique has not yet been applied to atomic negative ions, and, for atomic ions appears to offer no special advantages over other photodetachment methods, detailed descriptions will not be presented here. The reader is referred to the literature [147–149] for more complete information.

4.1.d. Laser Photodetached Electron Spectrometry

Full descriptions of the laser photodetached electron spectrometry (LPES) technique have been given in two papers [4, 5], and in this review we will only briefly discuss the apparatus, emphasizing those points that are of particular importance in the accurate determination of electron binding. A mass analyzed 680 eV negative ion beam is crossed with a monochromatic linearly polarized laser photon beam (4880 Å). Electrons photodetached in a small (0.0063 sr) solid angle perpendicular to the crossed beams are collected and energy analyzed by a hemispherical electrostatic analyzer with resolution of approximately 50 meV.

Since the photon momentum $h\nu/c$ is negligible in comparison to the ion, atom, and electron momenta involved, the basic energy balance equation can be written

$$h\nu - \text{EA} = \Omega_\text{L} + \text{E}_\text{cp} + \frac{m}{M}W - 2\left(\frac{mW\Omega_\text{L}}{M}\right)^{1/2}\sin\phi, \quad (10)$$

where $h\nu$ is the photon energy, EA is the energy difference between the initial negative ion state and the final atom state, Ω_L is the kinetic energy of the detached electron in the laboratory frame, m is the electron mass, M is the ion mass, W is the negative ion kinetic energy, ϕ is the angle between the negative ion velocity vector and

the electron collection direction (90° in this case), and E_{cp} is the contact potential difference between the interaction region and the electron energy analyzer. The last two terms are kinematic corrections arising from the fact that the detected photoelectrons must be slightly backscattered in the center-of-mass frame in order to enter the detector. The angularly dependent term vanishes for collection perpendicular to the ion beam, and need be considered only for error-analysis purposes. Under the conditions of this experiment, the kinematic correction is numerically 380 meV/amu, and represents an important correction in the determination of electron binding energies in almost all cases. To eliminate the effect of the essentially unknown contact potential difference, all electron affinities are measured with respect to an atom whose electron affinity is known accurately. To obviate the effect of a time varying contact potential, both the reference ion and the unknown ion are studied alternately on a time scale (1/60 s) short compared to that in which the contact potential can change significantly.

For the determination of the energy difference between two detached electron peaks, the 50 meV wide peaks can be fitted using standard least-squares techniques, and the energy *difference* can be determined to approximately 1 meV in most cases. There is a small nonlinearity in the energy scale of the analyzer (probably due to the fact that the electron energy analyzer employs a virtual entrance slit), but this effect has been thoroughly studied, and contributes uncertainties of less than 0.5 percent of the energy difference between the two detached electron peaks.

Using a second ion as the reference ion, the basic working equation for determining electron binding energies becomes

$$EA(2) = EA(1) + (\Omega_1 - \Omega_2) + mW\left(\frac{1}{M_1} - \frac{1}{M_2}\right), \quad (11)$$

where 1 and 2 refer to the reference ion and the unknown ion, respectively. Thus any future additive correction to the accepted value of the electron affinity of the reference ion can similarly be added to all vertical detachment energies and electron affinities determined via this technique. For this reason the reference ion is given for all LPES determinations reported in this review.

As with all experimental techniques, LPES has significant advantages and disadvantages when compared with other techniques. The principal disadvantage of LPES is that the basic measurement relies upon an *absolute* measurement of the energy difference between two groups of detached electrons, whereas the principal measurement in the photodetachment threshold technique is of an optical wavelength. Thus, the threshold measurements can be much more accurate than the LPES determinations, which at present are limited to a few millielectron volts. The 50 meV wide detached electron peaks also preclude the observation of fine structure in most cases, whereas such separations are easily seen in LPT studies.

A major advantage of LPES is that one is not limited to studying systems with binding energies greater than the minimum available photon energy and it has been possible to measure a number of EA's using LPES, which could not be obtained either with PT or LPT [2, 4–6, 129]. Another major advantage is that LPES essentially obtains only binding energies, whereas PT must measure an entire cross section over a significant wavelength region in order to determine binding energies. This means that the latter approach is more time consuming and difficult. Moreover, when a number of transitions are involved, the differential information available from LPES makes interpretation of the data far easier.

4.2. Plasma Absorption and Emission

Another technique that has yielded valuable information on negative ion binding energies is plasma photoabsorption [152–155] and photoemission [154, 156–164]. Photodetachment from negative halogen ions has been studied by measuring the absorption of a plasma that was created from alkali halides by shock-tube techniques. Berry et al. have been able to determine the electron affinities of the halogen atoms to within a few meV (see table 7) in this way [153]. The reverse process of radiative capture of plasma electrons by halogen atoms (radiative attachment) has been studied in shock-heated plasmas by Berry et al. [154] and Pietsch et al. [163]; they observe the photons emitted from the "affinity continua" around the long wavelength thresholds. The "cleanest" halogen affinity continua have been observed by Popp et al. [157–160], who studied the radiation emitted from the axis of a low-current cylindrical arc. Figure 5 shows a Cl⁻ absorption spectrum obtained by Berry et al. [152], and figure 6 shows the Cl⁻ affinity continua, as observed by Mück and Popp [159].

The behavior of the halide photoabsorption cross section near threshold is governed by the Wigner threshold law, $\sigma_{det} \propto k$ (where k is the momentum of the outgoing electron). By the use of microscopic reversability one obtains the energy-dependence of the radiative attachment cross section near threshold to be $\sigma_{att} \propto 1/k$, again for the case of radiative attachment into a p-shell. In order to determine the photon frequency dependence of the radiative attachment continuum (affinity continuum), it is necessary to convolve this energy-dependence with the low-energy portion of the electron speed distribution [$N(k)$] in the arc. If the low-energy distribution of electrons in the arc is Maxwellian, then $N(k) \propto k^2$, and both the dependence of the radiative attachment intensity $I(\nu)$ and the photoabsorption $A(\nu)$ on the photon frequency ν are expected to be the same,
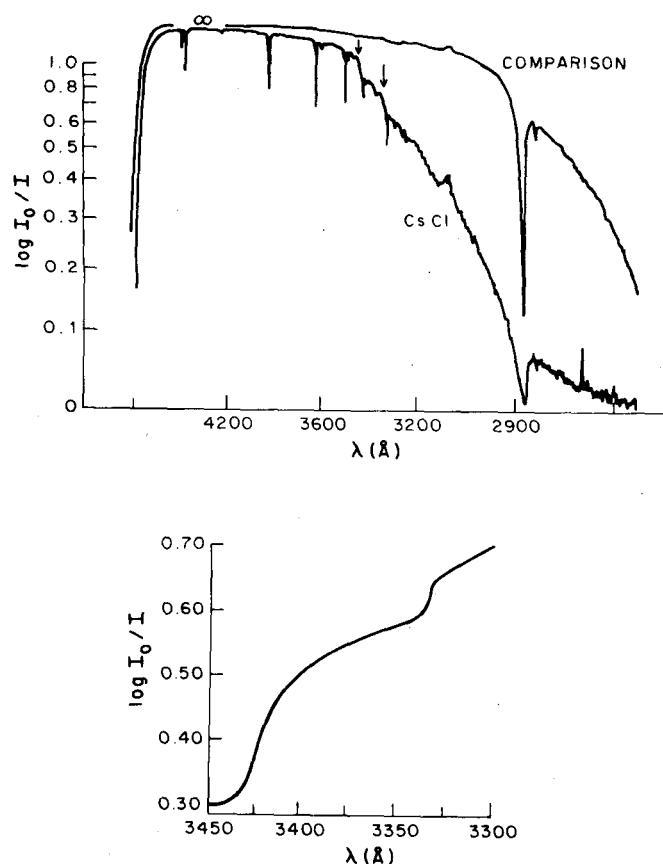
FIGURE 5. Upper figure: Microdensitometer tracing of absorption spectra in a CsCl seeded shock, showing onset of the continuous absorption of the Cl^- ion. The two extinction curves are with (lower) and without (upper) CsCl seeding. The difference between these curves is shown in the lower figure.

Lower figure: Extinction curve for Cl^- ion taken from the above spectrum and showing the two thresholds for $Cl\,^2P_{3/2+1/2}$. From Berry et al. [152] with permission.

FIGURE 7. Determination of the threshold wavelength from a Cl-affinity continuum at 6600 K (upper) and 8300 K (lower). The thresholds are determined in the manner first introduced by Berry et al. [152], and the threshold is indicated by the dot. Reprinted from Popp [35], with permission.

absorption, whereas in the radiative attachment case, the energy-dependence near threshold depends on knowledge of the electron speed distribution function at low energies. Since one can never see a true threshold, but must extrapolate, a functional form is very important.

In all studies carried out in plasmas to date, a considerable tail[2] extending to the long-wavelength side of the apparent threshold (due only to a minor degree to the finite optical resolution employed) was observed in the region of the expected sharp thresholds. Mück and Popp [159] studied the variation of their spectra as a function of electron temperature in the arc, as shown in figure 7 for 6600 K and 8300 K electron temperatures. One can clearly see the broadening of the onset at
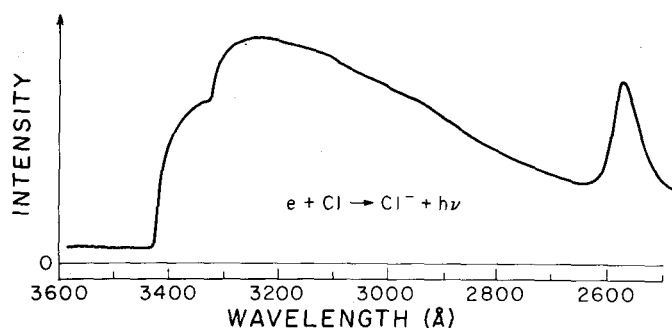

FIGURE 6. Direct reproduction of the chlorine-affinity continuum emitted from a low current Cl-arc, reproduced by permission from Muck and Popp [159].

$$\left.\begin{array}{c} I(\nu)d\nu \\ A(\nu)d\nu \end{array}\right\} \propto (\nu - \nu_{\text{thr}})^{1/2}d\nu \qquad (12)$$

in the immediate neighborhood of the threshold ν_{thr} for a particular transition. It must be emphasized, however, that the energy-dependence near threshold is a necessary result of simple physics in the case of photo-
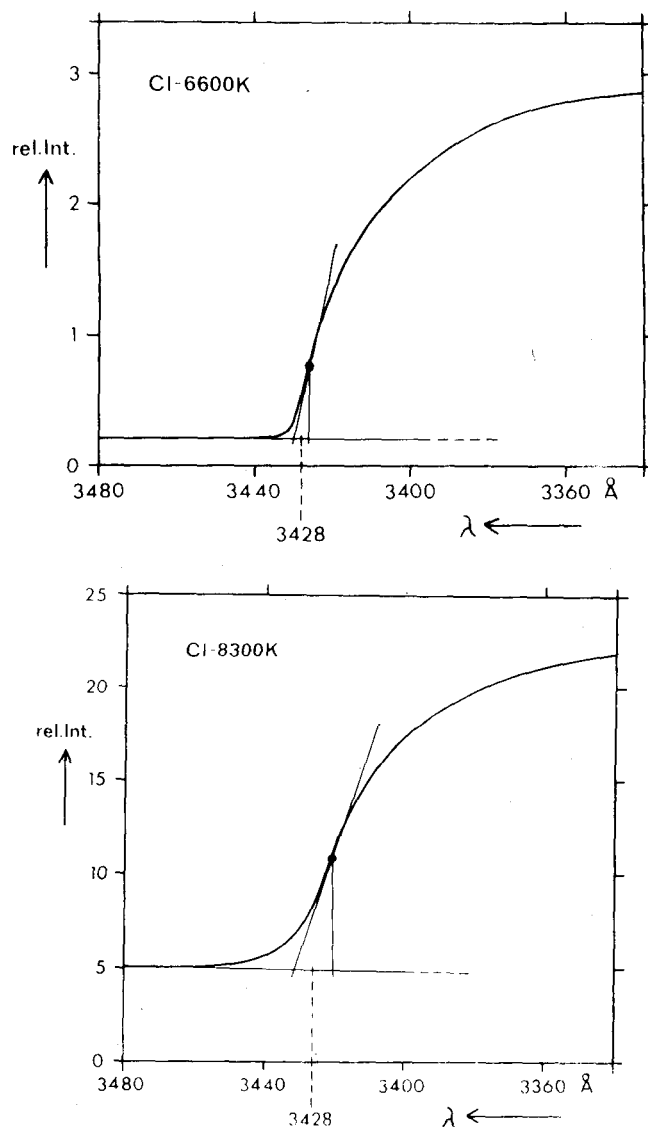
---

[2] This tail is commonly attributed to plasma effects which are not at all understood in detail. See discussion at the end of this section.

higher arc temperatures. They found that the threshold wavelength can be reproducibly determined for different arc conditions by an extrapolation method introduced by Berry et al. [152]. This method is indicated in figure 7, where λ_{thr} is taken as the midpoint between the turning point on the onset curve (the dot in fig. 7) and the linearly extrapolated threshold. Table 7 summarizes the results obtained with this method by the various authors using absorption or emission studies of the halogen atoms and the oxygen atom. For comparison, beam photodetachment data for I and O have been included. The results of either emission or absorption studies for the halogen atoms are found to be in good mutual agreement. In spite of the evidence given in figure 7 and the mutual agreement between the photoabsorption and photoemission studies, it is not certain at this point that the threshold extrapolation mentioned above is free from a systematic error of order millielectron volts.

The situation for EA(O) is somewhat less satisfactory. Berry et al. [156] deduced EA(O)=1.478(2) eV and found a value of (285 ± 10) cm^{-1} for the $O^-(^2P_{3/2,1/2})$ fine-structure separation in a radiative attachment measurement. Branscomb et al. [125] obtained 1.465(5) eV in a beam photodetachment experiment; their result is supported by a recent dye-laser photodetachment experiment on the threshold $O^-(^2P_{3/2}) \rightarrow O(^1D) + e$, which gave EA(O) = 1.462 $\left(\frac{6}{7} \right)$ eV [10]. These authors also determined the O^- fine-structure splitting as $(181 \pm$

4) cm^{-1} [8] through an isoelectronic extrapolation technique, which gave excellent agreement with the previous dye-laser photodetachment results for the similar splittings in S^- and Se^-. Very recently, Hoffmann and Popp [161] have also studied the affinity continuum of O, as emitted from a cylindrical arc. They located a clear onset at (8625 ± 10) Å which they ascribe to the $O(^3P_2) \rightarrow O^-(^2P_{1/2})$ transition. Unfortunately they were not able to locate with certainty the electron affinity transition $O(^3P_2) \rightarrow O^-(^2P_{3/2})$ because of interfering emission lines. It is possible that the onset seen by Hoffmann and Popp [161] corresponds to the threshold located at (8592 ± 6) Å by Berry et al. [156]. Both of these thresholds are ascribed to the $O(^3P_2) \rightarrow O^-(^2P_{1/2})$ transition in table 7.

If one accepts (8625 ± 10) Å as the threshold wavelength for $O(^3P_2) \rightarrow O^-(^2P_{1/2})$ and (181 ± 4) cm^{-1} for the O^- fine-structure splitting, then one derives EA(O)= 1.460(3) eV, in agreement with the beam photodetachment results. Further support for an affinity around 1.462 eV comes from a high resolution study by Dehmer and Chupka [165] of photoionization ion pair formation from O_2, giving EA(O)= (1.462 ± 0.003) eV as a lower limit; it is shown that at threshold the ion pair is produced with no more than about 5 meV kinetic energy and very probably with less. Finally, a fixed laser photodetached electron spectroscopy study, which compared the O^- and OH^- peaks, has yielded EA(O)= 1.459(9) eV [6], EA(OH) being known to within 2 meV from dye-laser photodetachment studies [12]. Our

TABLE 7.   Results of plasma photoabsorption and emission studies

Technique	Author	Atom-Negative Ion Transition in eV					
		$F(^2P_{3/2}) \rightarrow F^-$	$Cl(^2P_{3/2}) \rightarrow Cl^-$	$Br(^2P_{3/2}) \rightarrow Br^-$	$I(^2P_{3/2}) \rightarrow I^-$	$O(^3P_2) \rightarrow O^-(^2P_{3/2})$	$O(^3P_2) \rightarrow O^-(^2P_{1/2})$
Absorption by shock-produced plasma	Berry et al. [153]	3.398(2)	3.613(3)	3.363(3)	3.063(3)		
Emission from shock-heated plasma	Berry and David [154]		3.617(4)	3.360(4)	3.063(4)		
	Berry et al. [156]					1.478(2)	1.443(2)
	Popp et al. [158–162]	3.400(2)	3.616(3)	3.366(3)	3.062(2)		1.437(2)
Emission from shock-heated plasma	Pietsch and Rehder [163]		3.614(2)				
Photodetachment (beam)	Branscomb et al. [125, 128]				3.059	1.465(5)	
Recommended (see text)		3.399(3)	3.615(4)	3.364(4)	3.061(4)	1.462(3)	1.440(3)

conclusions from this discussion are that EA(O)=
1.462(3) eV, that the $O^-(^2P_{1/2})$ thresholds in table 7
are correct, and that the apparent $O^-(^2P_{3/2})$ threshold
obtained by Berry et al. [156] is an artifact.

Concerning our choice of the "best values" for the
electron affinity of halogen atoms, one might be inclined
to prefer the plasma absorption data over those obtained
in emission because the former do not depend on knowl-
edge of the plasma electron speed distribution. More-
over, the absorption studies were done on a much cooler
plasma (3000 K) [152, 153] than that used for emission
studies either by Pietsch et al. [163] or Popp et al.
[157–162] (electron temperature around 7000 K). A
higher electron temperature may result in a system-
atically shorter threshold wavelength because there are
relatively fewer slow electrons available for capture.
This effect might result in a higher number for the
electron affinity. As can be seen from the table, the
results obtained by Berry et al. [153, 164] in absorption
and by Popp et al. [158–162] in emission seem to indicate
(although their numbers are well within the mutual error
bars) a systematic difference of about 3 meV with the
radiative attachment results being higher. On the other
hand the emission results of Berry et al. [154] seem to
scatter around their absorption data rather than being
systematically different. The result of Pietsch and
Rehder [163] for Cl (emission measured behind the re-
flected shock wave, estimated temperature 6600 K)
agrees best with the absorption result of Berry et al.
[153]. We do not feel justified on the basis of the existing
evidence to attach real significance to the 2 to 3 meV
difference between Berry's absorption data [153] and
Popp's emission data [158–160, 162]. One should note
that the signal-to-noise quality of the data of Popp et al.
[158–160] appears to be the best of all of the above
measurements.

Concerning the comparison between the EA(I) re-
sults of Berry et al. [153, 154], Neiger [162], and
Steiner et al. [128] (again the numbers agree to within
their mutual error bars), we should point out that the
threshold expansion for the photodetachment cross
section that was used by Steiner, et al. in their fitting
procedure $[\sigma(k) = a(k + 5.6k^2)]$ does not have a
theoretical basis. As shown theoretically by O'Malley
[166] and supported by recent dye-laser photodetach-
ment studies of Se^- [8], a theoretical expansion of the
form ($k \ll 1$; k in a.u.)

$$\sigma(k) = ak(1 - bk^2 \, lnk - ck^2 - dk^3), \qquad (13)$$

where a, b, c, and d are positive constants, permits a
reasonable analytic description of the photodetach-
ment cross section in the range from threshold to
about 100 meV above threshold. Theoretically, there
should be no k^2 term in the threshold expansion, and
the first correction terms (of order k^3) to the basic
threshold law ($\sigma \propto k$) have negative signs [8, 166]. It
is likely that a threshold fit with a more realistic thresh-

old expansion would lead to a shorter threshold wave-
length in the data of Steiner et al. [128], since utilizing
the correct form of the threshold law [eq. (13)] essen-
tially amounts to imposing a steeper descent to the
threshold. On the basis both of this discussion and
Berry's plasma results [153, 154], we believe 3.061
eV to be the "best value" for EA(I).

It may be appropriate in concluding this section to
comment on the possible influence of the plasma on the
EA values obtained with plasma absorption or emission
techniques. Berry and Reimann [153] have discussed
this point at some length and conclude that Stark shifts
due to the ionic microfields and the corresponding shifts
of the photodetachment threshold are on the order
1 meV or less, whereas Stark broadening of the thresh-
old is expected to be a larger effect, in agreement with
the observed tails. In a more recent paper, Kobzev
[167] investigated quantitatively the effect of the
surrounding charged particles on negative ions in a
plasma. He derives a formula for the shift of the thresh-
old energy in plasma absorption experiments in terms
of the negative ion polarizability and the positive ion
density in the plasma, and applies this formula to I^-
plasma absorption, estimating a 10 meV lowering of the
threshold, in contrast to the conclusion of Berry and
Reimann [153]. Apparently unaware of the more
recent photodetachment data of Steiner et al. [128],
which yielded EA(I)=3.059(2) eV, Kobzev compared
Berry's number 3.063 eV [153, 154] with the earlier
(upper limit) photodetachment beam result of Steiner
et al. (3.076(5) eV) [127], concluding that his formula
described the level shift satisfactorily. It is clear from
the above that the level shift in Berry's I^--plasma
absorption was, if present, too small to be detectable
at the level of the quoted experimental uncertainties
of 2 to 3 meV.

4.3. Photodissociative Ion Pair Formation and Dissociative Electron Attachment

As described below, a simple energy balance criterion
can be used to determine electron affinities from either
photodissociative ion pair formation [e.g. 165, 168–174]
or dissociative electron capture by molecules [see e.g.
34, 37, 75, 175, 176]. In order to determine electron
affinities using dissociative electron capture, one must
study the energy dependence of reactions such as
$e + O_2 \rightarrow O^+ + O^- + e$ or $e + O_2 \rightarrow O^- + O$. There are
several difficulties in such experiments, which made
these methods obsolete once laser techniques became
available. The difficulties are as follows: i) monoener-
getic electrons are needed and the absolute electron
energy scale must be determined precisely; ii) the
kinetic energy of the ions must be measured and
corrected for Doppler broadening; iii) the target mole-
cule should be in its vibrational and rotational ground
state, or else a correction for the internal excitation
resulting from the gas temperature must be made.

The dissociative electron attachment technique suffers from much greater uncertainty than the photo-dissociative ion pair formation, because the former requires highly monoenergetic electrons of known energy, and the latter relies on optical excitation of the initial system. For this reason the discussion which follows will be couched solely in terms of the photo-dissociative processes; much larger uncertainties (of order 50 meV) are present in the dissociative electron capture method.

The observation of ion-pair formation in the course of photoabsorption by molecules

$$AB + h\nu \rightarrow A^- + B^+, \qquad (14)$$
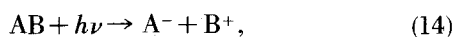
can yield precise information on EA(A) if the threshold behavior, including the rotational structure, can be sufficiently elucidated (e.g. by variation of the AB temperature), and if the kinetic energy of the ions is measured. We assume here that the ionization potential of B, IP(B), and the dissociation energy of AB, $D_0(AB)$, are arbitrarily well known from other experiments (which of course is often not the case at the milli-electron volt level). The quantity EA(A) is now simply determined by energy balance,

$$EA(A) = IP(B) + D_0(AB) - AP(A^-, B^+) + EK(A^-, B^+), \qquad (15)$$

where $AP(A^-, B^+)$ is the measured low-energy threshold for ion-pair formation in transitions originating from the vibrational-rotational ground state of AB, and $EK(A^-, B^+)$ is the center-of-mass energy of the ion pair at the threshold.

The essential experimental difficulty in determining accurate EA's in this manner lies in the precise determination of $EK(A^-, B^+)$, which is very hard to achieve to better than about 0.01 eV. For some cases it may be possible to *infer* that at threshold $EK(A^-, B^+) = 0$; insofar as this is not possible the numbers obtained for EA by photodissociative-ion pair production are lower bounds. Experimental ion-pair production studies of Br^- from Br_2 [168], I^- from I_2 [168], O^- from O_2 [165, 169], F^- from HF and F_2 [170, 172, 173] and H^- from H_2 [171, 220] have been reported in connection with atomic negative ion binding energies. These results are all included in the list of EA determinations in the last section of this review. The earlier results on Br^-, I^-, and O^- [168, 169] have been corrected, using more recent IP and D_0 values. The Br^- result by Morrison et al. [169] and the F^- result by Dibeler et al. [170] are in disagreement with the more precise data from plasma absorption and emission. As mentioned earlier, the EA's obtained for F by Popp [157, 158] and by Milstein and Berry [153b] using plasma techniques cannot be substantially in error, and one must look to the photodissociative ion-pair formation technique for the source of the disagreement. Chupka and Berkowitz [172, 173] have shown by both mass analysis and kinetic energy analysis of positive and negative ions

from HF and F_2 that the results of Dibeler et al. [170] are in error. The remaining discrepancy, the Br^- result by Morrison et al. [168] is not severe in view of the rather large error limit given there (EA(Br) = (3.51 ± 0.12) eV, corrected for new D_0 and IP values). The corresponding plasma determination is EA(Br) = (3.364 ± 0.004) eV [153, 159] (see table 7).

The photon energy width employed in the work of Morrison et al. [168] was 0.04 eV (FWHM), which was not adequate to permit the resolution of rotational transitions. Moreover the influence of the rotational energy in the Br_2 target on the ion-pair production efficiency is not discussed and the kinetic energy of the ions is not directly assessed (it is assessed indirectly by comparison with electron impact results carried out at different electron impact energies). We therefore believe that a somewhat lower ion-pair limit, which would be compatible with the EA obtained by the plasma studies, could in principle be obtained from the experimental data of Morrison et al. [168], if it were possible to do a full and complete analysis of such data.

The recent high resolution studies of photodissociative ion-pair formation from H_2 and D_2 by McCulloh and Walker [171] and Dehmer and Chupka [220] have come close to the desired situation. They both resolved different rotational transitions in the neighborhood of the ion-pair threshold and studied the ion-pair efficiency curve as a function of target gas temperature, including cool (110 K) para-hydrogen (more than 95 percent of H_2 molecules in $J = 0$, and the rest in $J = 2$). From the observed threshold McCulloh and Walker deduced the following lower bound: EA(H) ≥ (0.754 ± 0.002) eV [171]. With higher resolution, Dehmer and Chupka [220] were able to deduce EA(H) ≥ (0.7542 ± 0.0003) eV. Arguments were made (not including the fact that the results agreed with the very accurate EA calculated by Pekeris [56, 57], 0.75421 eV) that the center-of-mass energy of the ion pair at threshold must be very small, although it was not measured.

Another high resolution study was carried out by Dehmer and Chupka [165] on ion-pair formation from O_2. Their results indicate EA(O) = (1.462 ± 0.003) eV, in very good agreement with the beam photodetachment results and the less accurate photodissociative ion-pair production results of Elder et al. [169]. They also see what appears to be the $O^-(^2P_{1/2})$ production threshold, yielding a value for the $O^-(^2P_{3/2, 1/2})$ fine-structure splitting of about 22 meV.

In conclusion, one can say that photodissociative ion-pair production can indeed yield accurate atomic electron affinities if a careful analysis is made of the various effects mentioned above, and if evidence is given that both the negative and positive ions observed are indeed formed in the states assumed. However, at present, our somewhat limited knowledge of accurate dissociation energies of heavy diatomics precludes the use of this technique as an *accurate* method for obtaining electron affinities of heavy atoms.

4.4. Field Ionization

Binding energies of electrons in atoms or ions can in principle be determined by ionization in sufficiently strong well-defined electric fields E. In practice quantitative studies have until now been limited to binding energies less than 0.1 eV ($E \leqslant 500$ kV/cm) [177]. The field ionization method has been successfully applied [177] to the negative ions He$^-$(^{4}P$^\circ$), C$^-$(^{2}D), Si$^-$(^{2}P) and Al$^-$(^{1}D); a review of this and other work has been recently given by Il'in [177]. The interpretation of the experimentally obtained field ionization spectra (FIS) demands a careful theoretical analysis. Smirnov and Chibisov [178] have generalized the treatment of s-electron field ionization from atoms and ions in a discussion of FI of a particular (l,m) state. They used the one-electron approximation and assumed that the wave function of the electron inside the atom (ion) is not changed by the applied electric field. They employed their result to analyze field detachment of the p-electron in He$^-$($1s2s2p$)^{4}P$^\circ$, for which FIS had been obtained by Riviere and Sweetman [179].

Smirnov and Chibisov [178] interpreted these data essentially in terms of the more rapid decay of the $m=0$ component only and obtained $\epsilon = (60 \pm 5)$ meV for the binding energy ϵ of the p-electron. This number was found to disagree with a result [2] from laser-photodetached electron spectrometry on He$^-$(^{4}P$^\circ$), which yielded $\epsilon = (80 \pm 2)$ meV, and a maximum error limit of 8 meV. Later Oparin et al. [180] remeasured the He$^-$(^{4}P$^\circ$) FIS and found that it consisted, as expected from theory, of two lines corresponding to the ionization of $m=0$ and $|m|=1$. A careful analysis of these data with separate consideration of the two $|m|$ states yielded $\epsilon = (75 \pm 4)$ meV in satisfactory agreement [177, 180] with the photodetachment number. This result may be regarded as an experimental verification of the assumptions underlying the theory, at least for the case studied.

A comparison of the field ionization results for C$^-$(^{2}D), Si$^-$(^{2}P), and Al$^-$(^{1}D) with the recent photodetachment data again shows satisfactory agreement. It appears that field ionization is a suitable method for the determination of small electron affinities ($\leqslant 0.1$ eV), in spite of the facts that the data analysis depends heavily on theory and that a quantitative estimate of effects of systematic errors cannot be obtained in a direct way.

4.5. Surface Ionization; Thermochemical Methods

The fact that one can use surface ionization (SI) for the determination of binding energies in negative ions has been recognized for a long time [77, 116–118, 181–191], although a detailed appreciation of its advantages and drawbacks has only recently become possible, with the advent of reliable experimental data from photodetachment which could be compared [9, 10, 187] with the surface ionization data. Surface

ionization techniques have been discussed in detail by, among others, Zandberg and Ionov [181], Zandberg et al. [187], Smirnov [27, 28], Moiseiwitsch [26], and Page and Goode [31]. We shall restrict ourselves to the more recent studies relevant to atomic negative ions, especially to those of Zandberg et al. [183–187] and Scheer et al. [77, 116–118].

Essentially the surface ionization method is based on the assumption of thermodynamic equilibrium between a gas and a heated surface on which it is adsorbed. Then a definite relationship [187] exists between the number of electrons, atoms, positive ions, and negative ions being formed as the result of evaporation from the surface. Although this assumption is probably justified in many cases, it is very hard to test experimentally. The surface ionization studies of Zandberg and co-workers have employed two different techniques which we will call absolute surface ionization [183–187] and relative surface ionization studies [182–185].

In the absolute surface ionization of electron affinities [77, 183, 187], a single beam of atoms is incident upon a heated metal surface, and one measures the electron, positive ion, and negative ion currents as a function of surface temperature in order to determine both the work function of the surface and the electron affinity of the neutral, knowing the ionization potential of the atom. Assuming the validity of all the assumptions employed in this technique, one obtains the electron affinity of the atom, without recourse to any other electron affinity determinations. In the relative surface ionization technique [182–185], beams of two kinds of atoms impinge on a heated surface and one measures the ratio of ion currents of the two species as a function of temperature. Using this approach, one obtains a measurement of the *difference* in electron affinities between the two atomic species. It is possible [9, 10] that the requirement for thermodynamic equilibrium of the beams with the heated surface can be relaxed somewhat to simply a requirement that the two atomic species have very similar surface chemistries.

In the light of these remarks we note that the surface ionization method has yielded some results [77, 182, 183] that are in serious disagreement with the now firmly-established results obtained from photoabsorption. This disagreement is most pronounced in the absolute surface ionization measurements [77, 183] of electron affinities; for relative measurements of EA's the SI electron affinity differences between similar atoms are often found to be in good agreement with the photoabsorption results, e.g. for the halogen atoms [27] or for the noble metals Cu, Ag, and Au [182, 184]. The latter, on the other hand, were found to have EA's too high by ≈ 0.5 eV, as measured relative to I [182]. Very recently Zandberg et al. [187] have reevaluated the surface ionization techniques in light of the above disagreement. They conclude that the early [184, 182] absolute surface ionization measurement may have been

affected by systematic errors. They point out that the earlier work on I⁻ was under conditions such that some I⁻ ions were created in the gas phase, rather than on the surface. This effect would appear to account for only 0.05 eV of the 0.5 eV discrepancy. In the new absolute SI measurement [187], great care was taken to measure the work function of exactly that portion of the emitter from which ions were detected. Such precautions were not taken earlier, and the new absolute SI data on Ag and Au [187] are in good agreement with the photodetachment results. Zandberg et al. [187] have reevaluated all of the relative EA data based on these new results. It would appear that the SI technique can produce reliable results if extreme care is taken in the experimental process.

The method now preferred by Zandberg et al. [184, 185] over other methods involves a measurement of the ratio of negative and positive ion currents from a hot metal surface of known temperature upon impact of two different atomic beams, one of which serves as a calibration beam (commonly Ag). With this technique Zandberg et al. have measured the electron affinities of Sb, Bi, In [183], Cu, Sn, Pb [184], Si, and Ge [185] relative to that of Ag. Zandberg et al. used for EA(Ag) the value 1.9 eV [183] determined from their own absolute measurements, and the resulting electron affinities were in serious disagreement with other reliable electron affinity determinations in all cases where such determinations exist. If, however, instead of the absolute SI determination of EA(Ag), one uses the firmly established photodetachment value EA(Ag) = 1.30 eV [10], then the numbers for the above electron affinities are in good to fair agreement with all recent photodetachment results. This procedure has now been adopted by Zandberg [187]. Some of the remaining differences may possibly be attributed to the existence of excited bound negative ion states (as observed in Si, Ge, Sn, Pb among others) resulting in a somewhat lower value for the *effective* EA determined by Si.

The electron affinities of the refractory metals Nb, Mo, Ta, Re, and W have been studied by a special kind of SI, namely self-surface ionization (SSI), as developed by Scheer and coworkers [116–118]. With this technique one compares the ratio of sublimation of singly-charged positive and negative ions A⁺ and A⁻ from a heated surface made up of atoms A. Temperatures in the cases studied range from 1800 to 2600 K. The EA's are determined to within 0.1 to 0.3 eV (quoted error limits) from an isothermal measurement of the ratio of positive to negative ion sublimation rates. Since there are no other experimental data for comparison, the accuracy of this method is difficult to assess at present. The numbers so obtained are in reasonable agreement with an isoelectronic extrapolation (horizontal analysis), given the rather broad mutual error limits. The only exception is the case of Ta, for which IE predicts EA to be very close to zero, whereas SSI
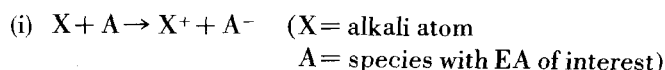
yields (0.8 ± 0.3) eV [118]. See table 6.
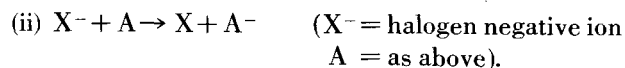
4.6. Other Experimental Methods

In addition to the experimental techniques discussed so far, several other methods have been employed for the determination of atomic electron affinities. We briefly mention here three forms of heavy particle collisions, involving either formation or destruction of the negative ion of interest. Bydin [74, 192] determined EA's for Na, K, Rb, and Cs by measuring the absolute cross section and its energy dependence (at a few kiloelectron volts) for resonant charge transfer of negative alkali ions in their parent atom gas and comparing the results with a theory developed by Firsov [193]. The EA's so obtained are too low by an appreciable amount; it is not clear in view of the difficulty of the experiment whether the discrepancy can be fully blamed on the theoretical model.

Relative negative ion destruction cross sections in the 10 to 40 keV region have been measured by Schmidt-Böcking and Bethge [78] for Li, B, C, O, F, S, Cl, Br, and I-negative ions in air (relative to H⁻ destruction in air, at the same ion velocity). From a simple model they derive a formula that connects the charge exchange cross sections (destruction cross sections) with the inverse electron binding energies, which allows them to calculate EA's by comparison with the EA for H. Their EA's so derived [78] for these atoms agree relatively well with the more precise photoabsorption results, except for the case of B [0.85(15) eV as compared to the LPES-value 0.28(1) eV].

The third method using heavy particle collisions is that of endoergic charge transfer (ECT), in which one determines the center-of-mass threshold kinetic energy for either

(i) $X + A \rightarrow X^+ + A^-$ (X = alkali atom
                                         A = species with EA of interest)

or

(ii) $X^- + A \rightarrow X + A^-$ (X⁻ = halogen negative ion
                                          A = as above).

For (i), X is chosen to have an ionization potential larger than EA(A), but still small enough to yield large cross sections for (i) above threshold [194–196]. Analogously, X⁻ is chosen to have EA(X) > EA(A) [197–199]. Cs was frequently used for (i), halogens for (ii). This method has yielded a number of valuable results for molecular species A and could also be worthwhile for determining atomic electron affinities.

5. Excited Long-Lived States in Atomic Negative Ions

While the earlier discussions have dealt almost exclusively with negative ions that are bound with

respect to the ground state of the parent atom, there is an important class of negative ions that are only bound relative to excited states of the parent atom, and yet live long enough ($\geqslant 10^{-6}$ s) to be detectable in mass spectrometers. Unfortunately very little quantitative information is available concerning these states, with the single important exception of $He^-(1s2s2p)\,{}^4P_J$.

Various atomic properties of this state have been studied in a series of papers by Novick et al. [200, 201]. These authors have measured the lifetimes of the $J=5/2$, $3/2$, and $1/2$ levels to be (500 ± 200), (10 ± 2), and (16 ± 4) μs, respectively [200, 201]. The EA of the parent atomic state, $He(2\,{}^3S)$, was determined by laser photodetached electron spectrometry (0.080(2) eV) [2] and by field ionization (0.075(4) eV) [177, 180]. Previous ab initio calculations have given lower bounds for this EA of 0.033 eV [202] and 0.069 eV [Weiss, cited in ref. 202].

Weiss [61] has treated excited states in Be^- and Mg^- with an ab initio CI method. The expected ground states of Be^- and Mg^-, $(ns)^2np$, have been shown to be unstable [26, 97, 101, 105], and Weiss showed [61] that the lowest lying Rydberg states $(ns)^2(n+1)s$ are also unstable. Weiss found, however, that the $(ns)(np)^2\,{}^4P^e$ states of Be^- and Mg^- are bound by 0.24(10) eV and 0.32(10) eV [61] with respect to their parent $nsnp\,{}^3P$. These states are metastable because autodetachment to the atomic ground state is spin-forbidden. It is very probable that Bethge et al. [203], using a mass spectrometer to detect Be^- and Mg^- ions produced in a Penning discharge-type ion source, have indeed seen these states. The same authors also detected Ca^-, Sr^-, and Ba^- [16], and it is not unlikely that all of these ions are in metastable states analogous in nature to the ^4P states of Be^- and Mg^-. Low resolution photodetachment data for Ca^- ions has been obtained by Heinicke et al. [114], but no definite conclusions on the energy of the negative ion state could be drawn. The laser photodetached electron spectrometry technique clearly provides the best way to study such ions.

Long-lived states of negative ions have been predicted semiempirically for quite some time for elements of the carbon group. Branscomb et al. [126] gave evidence for an excited bound state of C^-, ^2D; this state subsequently has been firmly established by field ionization [177, 204] and laser photodetached electron spectrometry studies [129], yielding a binding energy ϵ relative to $C(^3P_0)$ of about 35 meV.

Feldmann [134] detected an excited state in Si^-, with $\epsilon=0.56(4)$ eV. Kasdan, Herbst, and Lineberger [15] have recently used photodetached electron spectrometry to show that Si^- has two excited bound states, $SI^-(^2D)$ and $Si^-(^2P)$, with $\epsilon=0.523(5)$ and 0.029(5) eV, respectively. The latter state was also detected in field ionization studies [177] from which it was deduced that $\epsilon=0.037$ eV. From threshold photodetachment studies by Feldman and coworkers [42, 115] it is apparent that the ions Ge^-, Sn^-, and Pb^- all have at least one excited

state, presumably ^2D; their data have not permitted accurate evaluation of the term energies however. Again, it appears that photodetached electron spectrometry would provide a unique identification of these states.

In the fifth column of the periodic table, all atoms except N have at least one stable negative ion state (^3P). The first excited state is expected to be ^1D; if this state lies in the continuum, but below the atomic ^2D, it could be sufficiently long-lived to be detectable in a mass spectrometer since autodetachment to the ^4S atomic ground state is forbidden. For N^- it is known from ab initio calculations as well as semiempirical extrapolation studies, that both the $N^-(^1D)$ and the $N^-(^1S)$ states are bound by more than 0.5 eV relative to the parent atomic states, ^2D and ^2P, respectively. Both of these states are relatively long-lived because the only decay channels are forbidden, but no quantitative theoretical estimates of the lifetimes of these states are available. The only observation of N^- ions was in a double-charge exchange experiment by Fogel et al. [205], but no information on the ion states or lifetimes could be obtained. Several authors have attributed nitrogen plasma opacities [206–209] to the N^- ion.

Because of the importance of the N^- ion [205–209], we shall discuss its energetics in more detail. Table 8 summarizes the results of various ab initio and semiempirical calculations on the term splittings and ground state binding energies in N^- and C^-. For C^- comparison with experiment can be made. There is good agreement between the various results for the term splittings, which are not as sensitive to correlation effects as are the electron affinities. The IE results obtained with Edlén's formula [26] and the final numbers of Clementi and McLean [45] and of Schaefer and Klemm [83] are found to agree very well. We deduce the following "best" estimates for the N^- splittings:

$$N^-(^3P) - N^-(^1D) : 1.3(2) \text{ eV},$$
$$N^-(^3P) - N^-(^1S) : 2.6(2) \text{ eV}.$$

With the estimate $EA(N)=-0.07(8)$ eV one finds that $N^-(^1D)$ is bound by about 1.0 eV relative to $N(^2D)$ and that $N^-(^1S)$ is bound by about 0.9 eV relative to $N(^2P)$. This value for $EA(N)$ is also supported by recent $e-N$ scattering calculations by Burke et al. [218] who conclude $EA(N)=-0.06(5)$ eV.

The estimate $EA(N)=-0.07(8)$ eV has the following basis: The fact that to date it has not been possible to extract a beam of N^- ions from one of the many different ion sources used with success in negative ion work (even for beams of alkaline earths, Zn, Cd, and Hg negative ions! [16]) provides strong evidence that $N^-(^3P)$ is either unstable or bound by less than 10 meV (such as to make it very sensitive to destruction in weak electric fields). Ions with only slightly larger binding energies (20 to 40 meV) such as $C^-(^2D)$, $Si^-(^2P)$, NO^- have been fairly easily extracted from such ion sources. On the other hand, various recent ab initio calculations

TABLE 8.   Calculated term splittings in C^- and N^- and electron affinities of C and N (eV)

	$C^-(^4S)-C^-(^2D)$	$N^-(^3P)-N^-(^1D)$	$N^-(^3P)-N^-(^1S)$	$EA(C(^3P_0))$	$EA(N(^4S))$
(Restricted) Hartree-Fock [44]	1.80	1.50	3.68	0.55	−2.15
"Recommended"	1.23			1.268	−0.07(8)
Author and Method					
Bates & Moiseiwitsch [109] quadratic IE	1.40	1.34	2.77	0.92[a]	−0.56[a]
Moiseiwitsch [26] IE (Edlén formula)	1.29	1.28	2.60	1.24[b]	0.05[b]
Clementi & McLean [44] $HF + E_C$ extrapolation	1.25	1.23	2.59	1.17(6)	−0.27(11)
Schaefer et al. [83] CI + semiempirical estimate	1.35	1.33	2.67	1.24(10)	−0.21(10)
Öksüz & Sinanoğlu [84, 85] MET-correlation calculation and estimate	1.30	1.04	2.36	1.17	−0.45
Bagus et al. [86] MC HF	1.55	1.47	2.57	0.72	−1.44
Moser & Nesbet [47] Bethe-Goldstone calculation (orbital excitations; one and two particle terms)	1.27	1.35		1.46	0.19
Moser & Nesbet [48] Bethe-Goldstone calculation (configuration excitations)	1.48	1.40	3.0	1.21	−0.58

[a] G. Glockler [96]; quadratic IE.
[b] B. Edlén [97]; extended quadratic IE.

on $N^-(^3P)$, together with the best semiempirical estimates (see tables 3, 4, 8), lead us to the conclusion that $N^-(^3P)$ lies no more than 0.15 eV above $N(^4S)$. Therefore we estimate $EA(N) = -0.07(8)$ eV.

The first excited state of P^-, (^1D), is expected to lie very close to the $P(^4S)$ ground state; so far, this state has not been detected. Laser photodetached electron spectrometry on the transition $P^-(^1D) \rightarrow P(^2D)$ may be the best way to detect the presence of the ^1D state in a P^- beam. Even if the $P^-(^1D_2)$ state lies above $P(^4S)$, it could be sufficiently long-lived to be detected in a beam machine because autodetachment is spin-forbidden and mixing with $P^-(^3P_2)$ — in contrast to the situation in N^- — does not promote autodetachment, since $P^-(^3P_2)$ is bound, whereas $N^-(^3P_2)$ probably is not (see above). It should be mentioned here that a field ionization study [177] of P^- (produced by charge exchange of 100 keV P^+ ions in N_2) did not yield any attenuation of the P^- ion beam in fields up to 450 kV/cm. It would be worthwhile to study theoretically the field-ionization of a spin-forbidden transition such as $^1D \rightarrow {}^4S + e^-$.

Little is known about the ^1D states of As^-, Sb^-, and Bi^-. Isoelectronic extrapolation estimates indicate that these states lie about 1 eV above the (^3P) ground states.

Kaiser et al. [16] have observed the ions Zn^-, Cd^-, and Hg^- in a mass spectrometer employing an ion source of the type used by Heinicke. As in the case of the alkaline earth negative ions, one expects that these ions are in a metastable state, because the neutral atom closed-shell ground state makes it unlikely that stable negative

ions will be formed [102]. It is difficult to assess, however, whether the lowest Rydberg state $(ns)^2$ $(n+1)s$ may actually be bound and stable for heavier alkaline earths and for Zn, Cd, or Hg [102]. Isoelectronic extrapolations predict this state to be unstable for all of these atoms except Be [102]; for the latter a CI calculation by Weiss [61] indicates that it is unstable.

For several other atoms whose electron affinities have only been evaluated by isoelectronic extrapolation with results near or below zero, it is of considerable interest to know whether negative ions have been observed experimentally. Two important cases are Mn^- and Y^-, which have been observed by Kaiser et al. [16]. Unfortunately one cannot tell whether these ions are metastable or bound.

A discussion of long-lived states of negative ions would be incomplete without at least a brief comment on the recent mass spectrometric observation of doubly-charged negative ions, including O^{--}, Te^{--}, F^{--}, Cl^{--}, Br^{--}, and I^{--} by Baumann et al. [16, 38, 203]. In addition to these extensive observations, Ahnell and Koski [39] have recently reported observation of F^{--} ions. However, in the studies of Baumann et al. [38], the diagnostic techniques utilized to verify the identity and charge of the ions were by far the most complete of any of the observations. The detection techniques employed by Baumann et al. [38] involve the application of separate magnetic and electric fields, which should unambiguously separate collisionally-produced singly-charged ions from the doubly-

charged ions. Their observations showed that the "apparent" doubly-charged negative ion beam consisted of both doubly-charged negative ions and singly-charged atomic negative ions resulting from collisional dissociation of molecular ions. Variations of pressure in their apparatus showed that the doubly-charged negative ions had an extremely large collisional destruction cross section, as would be expected. Doubly-charged negative ion current in the nanoampere current range were reported [38] at ion energies of 10 to 20 keV, as extracted from a Penning ion source.

From a study of the data reported by Baumann et al. [38], it appears that all of the diagnostics which should be necessary to determine unambiguously the presence of doubly-charged negative ions were properly done. It should be pointed out, however, that by now several other research groups [210, 211] have unsuccessfully tried to produce and detect doubly-charged negative ions, including the unsuccessful attempts by Feldmann et al. [210], using the same ion source as Baumann et al. [38], to produce a beam of doubly-charged negative ions which could be used for photodetachment studies (i.e. a beam with currents $\gtrsim 10^{-9}$ A).

Further confirmation of the results of Baumann et al. [38] has to be forthcoming before the question of the existence of doubly-charged atomic negative ions with lifetimes $> 10^{-6}$ s can be viewed as satisfactorily answered.

Theoretically there is no concrete evidence that stable doubly-charged atomic negative ions exist. One may speculate that ions such as Te^{--} could approach stability. It is certain that some molecular ions in the gas phase will be capable of supporting a second negative charge. For example, the O^- ion sufficiently hydrated (perhaps with six H_2O molecules) would be able to support a second electron. Herrick and Stillinger [221] have recently discussed the state of computations of doubly-charged negative ions, specifically O^{--}, and find that the "ground state" is unstable. It is clear that these doubly-charged negative ions present a challenge to both theory and experiment which will be with us for some time.

6. Fine-Structure Splittings in Atomic Negative Ions

Table 9 summarizes values for negative ion fine-structure splittings. The energy differences between levels with the indicated total angular momentum J, measured relative to the ground level ($J = J_g$) are given in cm^{-1}. To date, experimental determinations of such splittings have been reported only for $He^-(^4P^\circ)$ [200, 201], $O^-(^2P)$ [156, 165], $S^-(^2P)$ [7], $Se^-(^2P)$ [8], and $Te^-(^2P)$ [212]. Mader and Novick [201] used a radio frequency technique to determine the fine-structure intervals in $^4He^-(^4P^\circ)$ and both the fine and hyperfine structure in $^3He^-(^4P^\circ)$. The fine-structure intervals listed for He^- are the determinations for the ^4He isotope.

As a result of the fact that EA(O) derived from radiative attachment emission spectra by Berry et al. [156] is incorrect, the fine-structure splitting deduced from this measurement for $O^-(^2P)$, 285(15) cm^{-1} [156], is also very probably in error. We prefer the value 181(4) cm^{-1} determined with a ratio isoelectronic extrapolation method (RIE) [8]. This method involves the extrapolation of ratios of fine-structure splittings along the isoelectronic sequence such as

$$\frac{\Delta E_{3/2-1/2}(O^-)}{\Delta E_{2-0}(O)}, \frac{\Delta E_{3/2-1/2}(F)}{\Delta E_{2-0}(F^+)}, \frac{\Delta E_{3/2-1/2}(Ne^+)}{\Delta E_{2-0}(Ne^{++})}, \cdots$$

These ratios are found to vary slowly with atomic number as can be seen for the oxygen and sulphur sequences in figure 8. A comparison of extrapolated values for $S^-(^2P)$ and $Se^-(^2P)$ gives very good agreement with the LPT data [8]. It should be mentioned that quadratic isoelectronic extrapolation (QIE) of the $O^-(^2P)$ splitting gives 230 cm^{-1} [100, 125]; comparison of results obtained with QIE for the accurately determined S^- and Se^- splittings indicates that the QIE numbers for negative ion splittings tend to be too high. The O^- splitting has also been extrapolated by use of Sommerfeld's formula, which essentially amounts to extrapolating the screening constant, a quantity that varies slowly with atomic number [105]; this extrapolation gives 182(5) cm^{-1} [8]. Recent photo ion-pair formation studies on O_2 by Chupka and Dehmer [165] corroborate the extrapolated splitting in $O^-(^2P)$. A summary of fine-structure splittings is given in table 9.
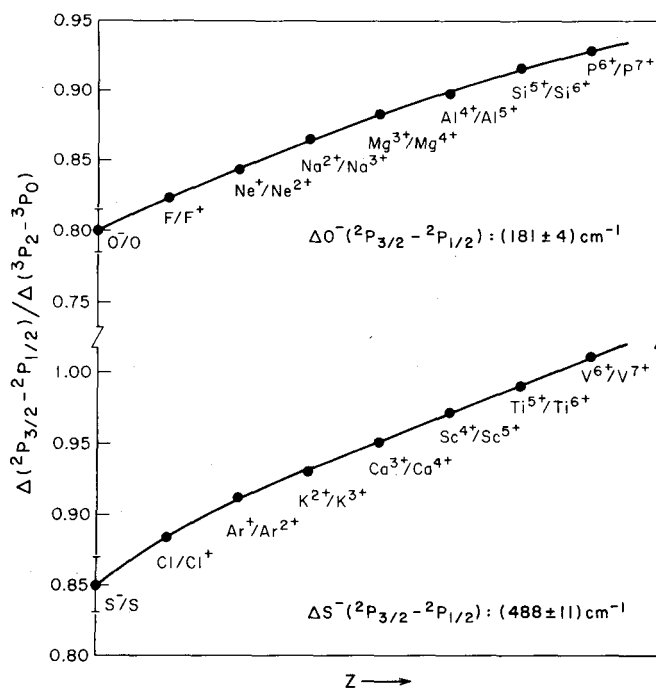

FIGURE 8. Isoelectronic extrapolations of fine-structure intervals in the S and O isoelectronic sequences. See text for details of the procedure employed. Reproduced from Hotop et al. [8], with permission.

TABLE 9. Fine-structure separations in negative ions

Negative ion	Fine-structure intervals $J_{ground} \to J_{excited}$	Separation (cm^{-1})	Method[a]	Reference: Comments[a]
He$^-$ (^{4}P$^\circ$)	5/2 → 3/2	0.027508(27)	rf technique	201
	5/2 → 1/2	.2888(18)	rf technique	201
B$^-$ (^{3}P)	0 → 1	4(1)	RIE	PP
	0 → 2	9(1)	RIE	PP
Al$^-$ (^{3}P)	0 → 1	26(3)	RIE	PP
	0 → 2	76(7)	RIE	PP
Ga$^-$ (^{3}P)	0 → 1	220(20)	RIE; QIE	PP; 102
	0 → 2	580(50)	RIE; QIE	PP; 102
In$^-$ (^{3}P)	0 → 1	680(70)	RIE; QIE	PP; 102
	0 → 2	1550(150)	RIE; QIE	PP; 102
Tl$^-$ (^{3}P)	0 → 1	3500(400)	RIE	PP, ^{3}P$_1$ possibly not bound
	0 → 2	5100(400)	RIE	PP, ^{3}P$_2$ possibly not bound
C$^-$ (^{2}D)	3/2 → 5/2	3(1)	LIE	PP
Si$^-$ (^{2}D)	3/2 → 5/2	7(2)	LIE	PP
Ge$^-$ (^{2}D)	3/2 → 5/2	160(30)	LIE	PP
Sn$^-$ (^{2}D)	3/2 → 5/2	800(200)	LIE	PP
P$^-$ (^{3}P)	2 → 1	190(20)	RIE; QIE	PP; 100
	2 → 0	280(30)	RIE; QIE	PP; 100
As$^-$ (^{3}P)	2 → 1	1100(200)	LIE; QIE	PP; 102
	2 → 0	1500(200)	LIE; QIE	PP; 102
Sb$^-$ (^{3}P)	2 → 1	2700(500)	LIE; QIE	PP; 102
	2 → 0	3000(500)	LIE; QIE	PP; 102
O$^-$ (^{2}P)	3/2 → 1/2	181(4)	RIE	8, 165
S$^-$ (^{2}P)	3/2 → 1/2	482(2)	LPT	7
Se$^-$ (^{2}P)	3/2 → 1/2	2279(2)	LPT	7
Te$^-$ (^{2}P)	3/2 → 1/2	5008(5)	LPT	212
Ni$^-$ (^{2}D)	5/2 → 3/2	1500(150)	QIE	102
Pt$^-$ (^{2}D)	5/2 → 3/2	10000(1000)	RIE; QIE	9, 102

[a] Abbreviations used:

rf   Radio frequency.
RIE   Isoelectronic extrapolation of ratios or fine-structure separations.
QIE   Quadratic isolectronic extrapolation.
LIE   Isoelectronic extrapolation from logarithmic plot.
PP   Present paper.

The splittings obtained with the technique labeled LIE were extrapolated graphically with either semi-log or log-log plots of the isoelectronic sequence. The errors estimated with this procedure were determined by comparison of the results of similar plots for S$^-$ and Se$^-$ with the LPT results. For some cases, values obtained with QIE were available for comparison. Experimental estimates for the fine-structure in P$^-$(^{3}P), As$^-$(^{3}P) and Sb$^-$(^{3}P) can be deduced from the PT data of Feldmann et al. [15]. Since in none of these latter cases could all three onsets [e.g. As$^-$(^{3}P$_{2,1,0}$) → As(^{4}S)] be isolated as a result of the moderate photon energy resolution,

we do not try to compare the apparent PT splittings with the given extrapolation results.

7. "Recommended Values" of Atomic Negative Ion Binding Energies

Table 10 summarizes what we consider the "best values" currently available for binding energies of atomic negative ion states. The organization of the table is as follows: atomic number, atomic designation; parent atomic states (ground state in most cases); negative ion state in question; binding energy of the appropriate negative ion state relative to the listed parent atomic state (>0 for bound states, <0 for continuum

states; this energy is the electron affinity if the ground state of the atom and the negative ion is listed); methods for those determinations of EA on which the choice is based, and finally, their respective references. The excited negative ion states listed (apart from fine-structure levels), bound or quasibound (i.e., autodetaching) correspond to long-lived states (lifetime $\geqslant 10^{-6}$ s) and are denoted (m), metastable. Shorter lived negative ion states have been omitted from the table. When the negative ion state is unknown or in doubt, a question mark has been placed together with the comment "detected" to indicate that negative ions of this Z have been experimentally observed, and are probably metastable.

TABLE 10. Summary of recommended atomic electron affinities (eV)

Z	Atom	Negative ion state[a]	EA(eV)	Method[b]	Reference no.[b]
1	H $1s$ $^2S_{1/2}$ (F = 0)	$1s^2$ $^1S_0$	0.754209(3)	Var. calc.	56; 57
2	He $1s^2$ $^1S_0$		<0	SE	102
2	He $1s2s$ 2^3S	$1s2s2p$ $^4P°$(m)	0.078(5)	LPES(H$^-$, D$^-$); FI	2; 177; 180
3	Li $2s$ $^2S_{1/2}$	$2s^2$ $^1S_0$	0.620(7)	LPES(K$^-$)	14
4	Be $2s^2$ $^1S_0$	$2s^22p$ ^2P	<0	SE	97; 100
		$2s^23s$ ^2S	<0	Calc.	61
4	Be $2s2p$ ^3P	$2s2p^2$ $^4P^e$ (m)	0.24(10)	CI Calc.	61
5	B $2p$ $^2P_{1/2}$	$2p^2$ $^3P_0$	0.28(1)	LPES(K$^-$)	40
6	C $2p^2$ $^3P_0$	$2p^3$ $^4S_{3/2}$	1.268(5)	LPES(O$^-$)	129
		$2p^3$ ^2D (m)	0.035(4)	FI	177; 204
7	N $2p^3$ $^4S_{3/2}$	$2p^4$ ^3P	$-0.07(8)$	Calc.; SE	PP
7	N $2p^3$ ^2D	$2p^4$ ^1D (m)	1.0(3)	Calc.; SE	PP
7	N $2p^3$ ^2P	$2p^4$ ^1S (m?)	0.9(3)	Calc.; SE	PP
8	O $2p^4$ $^3P_2$	$2p^5$ $^2P_{3/2}$	1.462(3)	PT; LPT; LPES(OH$^-$); IPF; P1E	125; 10; 6; 165; 161
9	F $2p^5$ $^2P_{3/2}$	$2p^6$ $^1S_0$	3.399(3)	P1A; P1E	153b; 157; 158
10	Ne $2p^6$ $^1S_0$		<0	SE	102
11	Na $3s$ $^2S_{1/2}$	$3s^2$ $^1S_0$	0.546(5)	LPES(K$^-$); LPT	14
12	Mg $3s^2$ $^1S_0$	$3s^23p$ ^2P	<0	SE; e scatt	97; 100; 101; 102; 222
12	Mg $3s^2$ $^1S_0$	$3s^24s$ ^2S	<0	SE	102
12	Mg $3s3p$ ^3P	$3s\,3p^2$ $^4P^e$ (m)	0.32(10)	CI calc.	61
13	Al $3p$ $^2P_{1/2}$	$3p^2$ $^3P_0$	0.46(3)	LPES	40
13	Al $3p$ $^2P_{1/2}$	$3p^2$ $^1D_2$ (m)	0.12(3)	LPES; FI	40; 177
14	Si $3p^2$ $^3P_0$	$3p^3$ $^4S_{3/2}$	1.385(5)	LPES(K$^-$)	21
14	Si $3p^2$ $^3P_0$	$3p^3$ $^2P_{3/2,5/2}$ (m)	0.523(5)	LPES(K$^-$)	21
14	Si $3p^2$ $^3P_0$	$3p^3$ $^2P_{1/2,3/2}$ (m)	0.029(5)	LPES(K$^-$)	21

TABLE 10. Summary of recommended atomic electron affinities (eV)—Continued

Z	Atom	Negative ion state[a]	EA(eV)	Method[b]	Reference no.[b]
15	P $3p^3$ $^4S_{3/2}$	$3p^4$ $^3P_2$	0.743(10)	PT; LPES(Na^-)	20; 40
15	P $3p^3$ $^4S_{3/2}$	$3p^4$ $^1D_2$	≈ 0	Calc.; SE	50; 109; 26
16	S $3p^4$ $^3P_2$	$3p^5$ $^2P_{3/2}$	2.0772(5)	LPT	7
17	Cl $3p^5$ $^2P_{3/2}$	$3p^6$ $^1S_0$	3.615(4)	P1A; P1E	153; 159; 163
18	Ar $3p^6$ $^1S_0$		< 0	SE	102
19	K $4s$ $^2S_{1/2}$	$4s^2$ $^1S_0$	0.5012(5)	LPT	14
20	Ca $4s^2$ $^1S_0$	$3d4s^2$ ^2D ?	< 0 ?	SE detected	110; 102 16; 114
21	Sc $3d4s^2$ $^2D_{3/2}$	$3d^24s^2$ ^3F	< 0	Calc., SE	51; 110; 102
22	Ti $3d^24s^2$ $^3F_2$	$3d^34s^2$ ^4F	0.2(2)	SE; calc.; detected	110; 102; 51; 16
23	V $3d^34s^2$ $^4F_{3/2}$	$3d^44s^2$ ^5D	0.5(2)	SE; calc.	110; 102; 51
24	Cr $3d^54s$ $^7S_3$	$3d^54s^2$ $^6S_{5/2}$	0.66(5)	PT	20
25	Mn $3d^54s^2$ $^6S_{5/2}$	$3d^64s^2$ ^5D ? (m)	< 0 ?	SE; calc. detected	110; 51; PP(102) 16
26	Fe $3d^64s^2$ $^5D_4$	$3d^74s^2$ ^4F	0.25(20)	SE; calc.	110; 51; PP(102)
27	Co $3d^74s^2$ $^4F_{9/2}$	$3d^84s^2$ ^3F	0.7(2)	SE; calc.	110; 51; PP(102)
28	Ni $3d^84s^2$ $^3F_4$	$3d^94s^2$ $^2D_{5/2}$	1.15(10)	PT	114
29	Cu $3d^{10}4s$ $^2S_{1/2}$	$3d^{10}4s^2$ $^1S_0$	1.226(10)	LPES(OH^-)	10
30	Zn $4s^2$ $^1S_0$	$4s^25s$ $^2S_{1/2}$ (?)	≈ 0	SE; detected	120; 16
31	Ga $4p$ $^2P_{1/2}$	$4p^2$ $^3P_0$	0.30(15)	SE; PT	102; 20
32	Ge $4p^2$ $^3P_0$	$4p^3$ $^4S_{3/2}$	1.2(1)	PT; SI(corrected)	20; 187
32	Ge $4p^2$ $^3P_0$	$4p^3$ ^2D	≈ 0.4	PT; SE	41; 102
33	As $4p^3$ $^4S_{3/2}$	$4p^4$ $^3P_2$	0.80(5)	PT	20
34	Se $4p^4$ $^3P_2$	$4p^5$ $^2P_{3/2}$	2.0206(3)	LPT	8
35	Br $4p^5$ $^2P_{3/2}$	$4p^6$ $^1S_0$	3.364(4)	P1A; P1E	153; 160
36	Kr $4p^6$ $^1S_0$		< 0	SE	102
37	Rb $5s$ $^2S_{1/2}$	$5s^2$ $^1S_0$	0.4860(5)	PLT	14
38	Sr $5s^2$ $^1S_0$	$4d5s^2$ ^2D (m?)	< 0	SE detected	110; 102 16
39	Y $4d5s^2$ $^2D_{3/2}$	$4d^25s^2$ ^3F	0.0(3)	SE; detected	110; PP(102); 16
40	Zr $4d^25s^2$ $^3F_2$	$4d^35s^2$ ^4F	0.5(3)	SE	110; PP(102)
41	Nb $4d^45s$ $^6D_{1/2}$	$4d^45s^2$ ^5D	1.0(3)	SSI; SE	118; 110; PP(102)
42	Mo $4d^55s$ $^7S_3$	$4d^55s^2$ $^6S_{5/2}$	1.0(2)	SSI; SE	118; PP(102)

TABLE 10. Summary of recommended atomic electron affinities (eV) — Continued

Z	Atom	Negative ion state[a]	EA(eV)	Method[b]	Reference no.[b]
43	Tc $4d^5 5s^2$ $^6S_{5/2}$	$4d^6 5s^2$ ^5D	0.7(3)	SE	110; PP(102)
44	Ru $4d^7 5s$ $^5F_5$	$4d^7 5s^2$ ^4F	1.1(3)	SE	110; PP(102)
45	Rh $4d^8 5s$ $^4F_{9/2}$	$4d^8 5s^2$ ^3F	1.2(3)	SE	110; PP(102)
46	Pd $4d^{10}$ $^1S_0$	$4d^9 5s^2$ $^2D_{5/2}$	0.6(3)	SE	110; PP(102)
46	Pd $4d^{10}$ $^1S_0$	$4d^{10} 5s$ $^2S_{1/2}$	?		
47	Ag $4d^{10} 5s$ $^2S_{1/2}$	$4d^{10} 5s^2$ $^1S_0$	1.303(7)	LPES(O$^-$)	10
48	Cd $4d^{10} 5s^2$ $^1S_0$	$5s^2 6s$ $^2S_{1/2}$	$\lesssim 0$?	SE; detected	102; 16
48	Cd $4d^{10} 5s^2$ $^1S_0$	$5s^2 6p$ ^2P	< 0	SE	102
49	In $5p$ $^2P_{1/2}$	$5p^2$ $^3P_0$	0.30(15)	SE; PT; SI (corrected)	102; 20; 183
50	Sn $5p^2$ $^3P_0$	$5p^3$ $^4S_{3/2}$	1.25(10)	PT; SI (corrected)	20; 187
50	Sn $5p^2$ $^3P_0$	$5p^3$ ^2D	0.4(2)	PT; SE	41; 102
51	Sb $5p^3$ $^4S_{3/2}$	$5p^4$ $^3P_2$	1.05(5)	PT	20
52	Te $5p^4$ $^3P_2$	$5p^5$ $^2P_{3/2}$	1.9708(3)	LPT; PT	212; 20
53	I $5p^5$ $^2P_{3/2}$	$5p^6$ $^1S_0$	3.061(4)	PT; P1A; P1E	128; 153; 154; 162
54	Kr $5p^6$ $^1S_0$		< 0	SE	102
55	Cs $6s$ $^2S_{1/2}$	$6s^2$ $^1S_0$	$0.4715\binom{5}{20}$	LPT; LPES(K$^-$)	14; 19
56	Ba $6s^2$ $^1S_0$	$5d6s^2$ ^2D (m?)	< 0	SE detected	PP(102) 16
57	La $5d6s^2$ $^2D_{3/2}$	$5d^2 6s^2$ $^3F_2$	0.5(3)	SE	PP(102)
58					
	Rare earths		$\lesssim 0.5$	estimate	102
71					
72	Hf $5d^2 6s^2$ $^3F_2$	$5d^3 6s^2$ ^4F	> 0	SE	PP(102)
73	Ta $5d^3 6s^2$ $^4F_{3/2}$	$5d^4 6s^2$ ^5D	0.6(4)	SSI; SE	118; PP(102)
74	W $5d^4 6s^2$ $^5D_0$	$5d^5 6s^2$ $^6S_{5/2}$	0.6(4)	SSI; SE	118; PP(102)
75	Re $5d^5 6s^2$ $^6S_{5/2}$	$5d^6 6s^2$ ^5D	0.15(10)	SSI; SE	118; PP(102)
76	Os $5d^6 6s^2$ $^5D_4$	$5d^7 6s^2$ ^4F	1.1(3)	SE	PP(102)
77	Ir $5d^7 6s^2$ $^4F_{9/2}$	$5d^8 6s^2$ ^3F	1.6(2)	SE	PP(102)
78	Pt $5d^9 6s$ $^3D_3$	$5d^9 6s^2$ $^2D_{5/2}$	2.128	LPT	9
79	Au $5d^{10} 6s$ $^2S_{1/2}$	$5d^{10} 6s^2$ $^1S_0$	2.3086(7)	LPT	9
80	Hg $6s^2$ $^1S_0$	$6s^2 7s$ $^2S_{1/2}$	< 0	SE	102
		$6s^2 6p$ $^2P_{1/2}$? (m)	< 0	SE; e$^-$ scatt. detected	102; 213 16
81	Tl $6s^2 6p$ $^2P_{1/2}$	$6p^2$ $^3P_0$	0.3(2)	SE; PT	102; 20

TABLE 10. Summary of recommended atomic electron affinities (eV)—Continued

Z	Atom			Negative ion state[a]	EA(eV)	Method[b]	Reference no.[b]
82	Pb	$6p^2$	$^3P_0$	$6p^3$ $^4S_{3/2}$	1.1(2)	SI (corrected); PT; SE	184; 187; 115; 102
82	Pb	$6p^2$	$^3P_0$	$6p^3$ $^2D_{3/2}$	>0	PT	115
83	Bi	$6p^3$	$^4S_{3/2}$	$6p^4$ $^3P_2$	1.1(2)	SI (corrected); PT	183; 187; 20
84	Po	$6p^4$	$^3P_2$	$6p^5$ $^2P_{3/2}$	1.9(3)	SE	102; 113
85	At	$6p^5$	$^2P_{3/2}$	$6p^2$ $^1S_0$	2.8(2)	SE	102
86	Rn	$6p^6$	$^1S_0$		<0		102

[a] (m) indicates metastable.
[b] Abbreviations used:

    PT   Photodetachment threshold (beam).
    LPT   Tunable laser photodetachment threshold (beam).
    LPES   Laser photodetachment electron spectrometry.
    SE   Semiempirical extrapolation (IE and/or HA).
    P1A, P1E Plasma absorption, plasma emission.
    SI   Surface ionization.
    SSI   Self-Surface Ionizations.
    FI   Field Ionization.
    PP(102) Present paper (Zollweg horizontal analysis reevaluated).

The error bars assigned are our best estimates of the probable accuracy and reflect the following:

1) the uncertainty of that single experiment viewed as being most reliable and accurate;

2) combined errors if the number given is based on more than one experiment, with subjective weights given to those experiments considered by us to be most reliable;

3) combined errors if the number given is based both experimental and semiempirical or theoretical information; in this case preference has been given to experimental data;

4) estimated errors for numbers which are based only on semiempirical extrapolation. The error limits are expected to include the "true" value at the 90 percent confidence level *provided* that the actual ground state configuration of the negative ion is that which we have assigned.

Where laser photodetachment data are available (with the exception of several excited states of negative ions) we have selected those data as being most reliable. In cases for which there are two sets of laser photodetachment data (the heavier alkalis), the quoted results agree to within the respective error bars, but we have given heavier weight to the tunable laser photodetachment results, which are generally more accurate. Where "clean" photodetachment data are available, all of the photodetachment results agree to within the stated uncertainty limits. The exceptions to these statements are limited to cases of overlapping thresholds, misidentification of thresholds, or use of incorrect threshold law forms in extrapolation.

For those recommended electron affinities based upon laser photoelectron spectrometry (LPES), one must recognize that the EA determinations are relative to some calibration ion whose EA is known from another source. The ion used in calibration is listed in parentheses, i.e., LPES(K⁻), and the EA of the reference is not necessarily that used in the original paper, but instead is that given for the reference in this table. This means that, should the "best" value for EA of a reference ion change in the future, all EA determinations based upon that ion and listed in this table can be immediately updated.

All binding energies are given in electron volts. We have used the following conversion factors: 1 atomic unit = 27.210 eV; 1 eV = 8065.479(21) cm^{-1}, as given by Cohen and Taylor [214]. At this point we will proceed to discuss in somewhat more detail the arguments that led to the above list of recommended values for binding energies. The negative ions of the main group elements will be discussed by columns, and the three long series horizontally.

Group IA (alkali negative ions including H⁻). All of the atoms in Group IA have one stable negative ion state, $^1S_0$. For the case of atomic hydrogen, it is clear that theory is ahead of experiment, and preference must be given to the theoretical determinations [56–58]. However, recent photodetachment studies by Feldmann [219] yielding EA(H) = (6081 ± 16) cm^{-1} and ion pair formation studies by Dehmer and Chupka [220] yielding EA(H) = (6083.0 ± 2.4) cm^{-1} are beginning to test the calculated values.

The listed EA(H) is that of the lower hyperfine level in H(F = 0); the given uncertainty is an estimate of the combined errors in the relativistic and radiative contributions to EA(H).

For the EA of the alkali atoms, the laser photodetach-

ment values [14], in some cases being a weighted average of results from the two different laser techniques, were chosen. In all cases, the results agreed to within the individual error limits. The less accurate threshold photodetachment results of Feldmann et al. [20, 79] are in good agreement with the laser photodetachment numbers, but these determinations were not used in the final selection.

Group IIA (alkaline earth ions). Although not known with certainty, it is likely that the stable negative alkaline earth ions do not exist, and that the alkaline earth negative ions detected by Bethge et al. [16, 203], are metastable, probably in the lowest $nsnp^2$ ^4P state. Burrow and Comer [222] have recently reported an electron scattering resonance in the e–Mg system at 0.15 eV, which is associated with the $3s^23p$ ^2P state of Mg. The most likely candidate for a stable negative ion is Ba$^-$, for which the $5d6s^2$ state is extrapolated to be unstable by only about 0.5 eV. This case is similar to that of Y$^-$, which is also predicted to be unstable by the same amount, and yet has been observed. It is conceivable that the horizontal analysis is wrong by energies of order 0.5 eV for the elements adjacent to the alkali atoms in the long series, since rather large deviations from the straight line behavior of the $d^ks^2 \rightarrow d^ks$ energy difference are observed in this region of the neutral atom long series ($q = 0$). The correction we apply amounts to half the deviation observed in the horizontal series ($q = 0$) and may underestimate the deviation possible for negative ions. The near degeneracy of different subshells may be particularly important in negative ions and produce "atypical" behavior when compared with that in the neutral or positive ion series.

Group IIIA. Photodetachment experiments have now been carried out on all of these negative ions, with accurate data now available for B$^-$(^3P) and Al$^-$(^3P, ^1D), and *upper bounds* of about 0.5 eV for the binding energy in Ga$^-$, In$^-$, and Tl$^-$. The electron affinities chosen for the latter three elements are based on these bounds and the horizontal analysis by Zollweg, including a comparison of his predictions for other atoms with well-known EA's, and following the trends of the observed deviations as one proceeds toward Group IIIA.

Group IVA. The numbers given are based on photodetachment results, whenever their interpretation was conclusive. The EA(C) is based on an unpublished measurement made by Bennett and Hall using LPES; the comparison of the C$^-$ and O$^-$ electron energy spectra gave EA(C) = EA(O) − 0.194(2) eV. The uncertainty stated includes the estimated error arising from the unresolved fine structure hidden in both detached electron peaks. Using EA(O) = 1.462(3) eV, one obtains EA(C) = 1.268(5) eV. The earlier, less accurate, results of Branscomb et al. (1.25(3) eV) and Hall and Siegel (1.27(1) eV) are in agreement with this determination.

Bennett [215] also restudied the C$^-$(^2D) $\rightarrow$ C(^3P) transition, for which Hall and Siegel had given a pre-

liminary value of 0.062 eV for the C$^-$(^2D) binding energy, compared with the value 0.035(4) eV derived from C$^-$(^2D) field ionization studies. The energy scale compression in the LPES apparatus was not appreciated at this time, and the 0.062 eV value is very likely quite high. Unfortunately, Bennett's ^2D data were not as accurate as typical of the LPES data as a result of poor statistics and a small number of counts in the ^2D detached electron peak; nonetheless the analysis yielded a C$^-$(^2D) binding energy of 0.05(2) eV. We have chosen the field ionization result as being the best measurement of the binding energy of this state. It should be pointed out, however, that a precise independent measurement of this quantity would be very worthwhile in order to test the validity of the one-electron approximation used in the interpretation of the field ionization data, which in this case was applied to a p^3 configuration.

In the similar case of Si$^-$(^2P), LPES yields 0.029(5) eV, in reasonable agreement with the 0.037 eV deduced from the Si$^-$ field ionization studies. The Si$^-$ ion has three bound electronic states of the p^3 configuration, ^4S, ^2D, and ^2P. The observation of transitions from all three negative ion states, populated to varying degrees depending upon ion source conditions, to states of the neutral atom, provides an unambiguous determination of their respective binding energies.

Photodetachment (PT) experiments on Ge$^-$ and Sn$^-$ provide clear evidence for the presence of (at least) one excited bound negative ion state, ^2D, but to date only the binding energy of the ground state has been deduced. We have listed estimates for the ^2D-state binding energy in Ge$^-$ and Sn$^-$; they are based on inspection of the low energy photodetachment onsets, and on isoelectronic extrapolation results of Zollweg.

The Pb$^-$ photodetachment cross section obtained by Kaiser et al. did not allow a straightforward interpretation. Electron affinities of about 0.34 eV or 1.21 eV would provide an explanation of the data obtained in the photon energy range 0.5 to 3 eV. The surface ionization result 1.05(8) eV (relative to EA(Ag)=1.30 eV) and Zollweg's HA estimate of 1.03 eV support the higher value. We have thus chosen EA(Pb)=1.1(2) eV as the best estimate.

Group VA. The selected values for electron affinities of P, As, and Sb are based on recent photodetachment threshold data, and the result for P has been corroborated by LPES. A detailed discussion of the ^1D negative ion states has been given in section 5. The situation for the determination of EA(Bi) is similar to that discussed previously for Pb. The number given is a compromise between a surface ionization result (relative to Ag), the poorly understood photodetachment data, and an estimate based upon horizontal analysis.

Group VIA. The laser photodetachment (LPT) experiments have yielded precise values for the electron affinites of S, Se and Te; for Te, the broad range PT data of Feldmann et al. [20, 115] makes the narrow

range LPT data identification unique. The quantity EA(O) is least well known in this group (apart from Po), but the values EA(O)=1.462(3) eV, based upon five independent experiments, is sufficiently accurate for many purposes. A detailed discussion of the manner in which this value was arrived at was given in section 4.2. In order to further improve upon this situation, LPT experiments in the neighborhood of 8500 Å are needed to yield EA(O) and the O⁻ fine-structure splitting with millielectron volt accuracy. The estimate given for EA(Po) is based on two semiempirical values and the vertical trend for group VIA electron affinities.

Group VIIA (halogen negative ions). The numbers given are based on plasma absorption and emission experiments by Berry et al. and Popp et al. and on one PT experiment on I⁻. A detailed discussion of the problems faced in the proper determination of the threshold wavelength in the plasma data was given in section 4.2. It is our feeling that the error bars stated are extended sufficiently to encompass the "true" EA, even given the present uncertainty in the nature of plasma effects on thresholds.

The three long series (transition metals). Accurate experimental numbers (uncertainty less than 0.1 eV) are available only for Cr, Ni, Cu, Ag, Pt, and Au. The SSI technique provided values for Nb, Mo, Ta, W, and Re with estimated error limits ranging from 0.1 to 0.3 eV. Most of the numbers given here are based upon horizontal analysis between the alkali and noble metal negative ions, as described in section 3. In some cases these estimates were slightly changed in connection with other work (Clementi, Charkin and Dyatkina; experimental evidence, "detected") to yield what we believe are better final estimates. Almost nothing is known about the negative ions of the rare earth elements; Zollweg estimates that either stable negative ions do not exist, or their electron affinity is below about 0.5 eV.

8. Conclusions

In this article we have attempted to summarize the present state of our knowledge of binding energies in atomic negative ions. It is clear that developments in ion source and tunable laser technology over the past five years have greatly increased our knowledge of this subject. The electron affinities of the atoms of the main body of the periodic table are reasonably well known, and it is now apparent that excited states of negative ions, which were once thought to be very rare, are in fact quite common for atoms in the center of the periodic table.

In contrast, the long series, the lanthanides, and the actinides are virtually unstudied experimentally. It can be hoped that the technique of laser photodetached electron spectrometry will be able to unravel many of the remaining questions concerning these ions in the near future. Only at this point will we be able to assess quantitatively how accurate the various extrapolation techniques are.

1 H 0.7542							2 He <0
3 Li 0.620	4 Be <0	5 B 0.28	6 C 1.268	7 N ≤0	8 O 1.462	9 F 3.399	10 Ne <0
11 Na 0.546	12 Mg <0	13 Al 0.46	14 Si 1.385	15 P 0.743	16 S 2.0772	17 Cl 3.615	18 Ar <0
19 K 0.5012	20 Ca <0	31 Ga 0.3	32 Ge 1.2	33 As 0.80	34 Se 2.0206	35 Br 3.364	36 Kr <0
37 Rb 0.4860	38 Sr <0	49 In 0.3	50 Sn 1.25	51 Sb 1.05	52 Te 1.9708	53 I 3.061	54 Xe <0
55 Cs 0.4715	56 Ba <0	81 Tl 0.3	82 Pb 1.1	83 Bi 1.1	84 Po 1.9	85 At 2.8	86 Rn <0

FIGURE 9. Recommended electron affinities for the ground state atoms of the main body of the periodic table. These values are obtained from table 10; the width of solid bar below each element is proportional to the percentage uncertainty in the electron affinity. For elements with no bar shown (e.g., S), the uncertainty is too small to be represented in this fashion. See table 10 for more details.

21 Sc <0	22 Ti 0.2	23 V 0.5	24 Cr 0.66	25 Mn <0	26 Fe 0.25	27 Co 0.7	28 Ni 1.15	29 Cu 1.226	30 Zn <0
39 Y ≈0	40 Zr 0.5	41 Nb 1.0	42 Mo 1.0	43 Tc 0.7	44 Ru 1.1	45 Rh 1.2	46 Pd 0.6	47 Ag 1.303	48 Cd <0
57 La 0.5	72 Hf <0	73 Ta 0.6	74 W 0.6	75 Re 0.15	76 Os 1.1	77 Ir 1.6	78 Pt 2.128	79 Au 2.3086	80 Hg <0

FIGURE 10. Periodic chart showing best electron affinities for the electrons of the three long series. The width of the solid bar is proportional to the percentages uncertainty, as in figure 9. See table 10 for details.

Figures 9 and 10 are periodic tables that summarize the present knowledge of the electron affinities of the elements relative to the ground state atom. The width of the solid bar below each element is proportional to the percentage uncertainty in the electron affinity determination, as obtained from table 10. For detailed information, these figures must be supplemented with that table.

9. Acknowledgments

10. References

[1] a) W. C. Lineberger in *Chemical and Biochemical Applications of Lasers*, Vol. I, C. B. Moore, Ed. (Academic, New York, 1974), pp. 71–101.
     b) W. C. Lineberger in *Energy, Structure and Reactivity*, D. W. Smith and W. B. McRae, Eds. (Wiley, New York, 1974), pp. 333–355.
     c) W. C. Lineberger in *Laser Spectroscopy*, R. Brewer and A. Mooradian, Eds. (Plenum, New York, 1974) pp. 581–595.

[2] B. Brehm, M. A. Gusinow, and J. L. Hall, Phys. Rev. Lett. **19**, 737 (1967).

[3] J. L. Hall and M. W. Siegel, J. Chem. Phys. **48**, 943 (1968).

[4] M. W. Siegel, R. J. Celotta, J. L. Hall, J. Levine, and R. A. Bennett, Phys. Rev. A **6**, 607 (1972).

[5] R. J. Celotta, R. A. Bennett, J. L. Hall, M. W. Siegel, and J. Levine, Phys. Rev. A **6**, 631 (1972).

[6] R. J. Celotta, R. A. Bennett, and J. L. Hall, J. Chem. Phys. **60**, 1740 (1974).

[7] W. C. Lineberger and B. W. Woodward, Phys. Rev. Lett. **25**, 424 (1970).

[8] H. Hotop, T. A. Patterson, and W. C. Lineberger, Phys. Rev. A **8**, 762 (1973).

[9] H. Hotop and W. C. Lineberger, J. Chem. Phys. **58**, 2379 (1973).

[10] H. Hotop, R. A. Bennett, and W. C. Lineberger, J. Chem. Phys. **58**, 2373 (1973).

[11] W. C. Lineberger and T. A. Patterson, Chem. Phys. Lett. **13**, 40 (1972).

[12] H. Hotop, T. A. Patterson, and W. C. Lineberger, J. Chem. Phys. **60**, 1806 (1974).

[13] H. Hotop, T. A. Patterson, and W. C. Lineberger, Advan. Mass Spectrom. **6**, 287 (1974).

[14] T. A. Patterson, H. Hotop, A. Kasdan, D. W. Norcross, and W. C. Lineberger, Phys. Rev. Lett. **32**, 189 (1974).

[15] A. Kasdan, E. Herbst, and W. C. Lineberger, *Fourth International Conference on Atomic Physics: Abstracts of Contributed Papers*, Heidelberg, July 22–26, 1974, pp. 246–248.

[16] H. J. Kaiser, E. Heinicke, H. Baumann, and K. Bethge, Z. Physik **243**, 46 (1971).

[17] E. Heinicke, K. Bethge, and H. Baumann, Nucl. Instr. Meth. **58**, 125 (1968).

[18] H. Baumann, K. Bethge, and E. Heinicke, Nucl. Instr. Meth. **46**, 43 (1967).

[19] A. Kasdan and W. C. Lineberger, Phys. Rev. A **10**, 1658 (1974).

[20] D. Feldmann, R. Rackwitz, E. Heinicke, and H. J. Kaiser, Phys. Lett. **45A**, 404 (1973).

[21] A. Kasdan, E. Herbst, and W. C. Lineberger, J. Chem. Phys. **62**, 541 (1975).

[22] H. S. W. Massey, *Negative Ions* (Cambridge University Press, London, 1950).

[23] H. O. Pritchard, Chemical Reviews **52**, 529 (1953).

[24] N. S. Buchel'nikova, Usp. Fiz. Nauk. **65**, 351 (1958).

[25] L. M. Branscomb, in *Atomic and Molecular Processes*, D. R. Bates, Ed. (Academic, New York, 1962), pp. 100–140.

[26] B. L. Moiseiwitsch, Advan. Atomic and Mol. Phys. **1**, 61 (1965).

[27] B. M. Smirnov, High Temperature **3**, 716 (1965).

[28] B. M. Smirnov, *Atomic Collisions and Elementary Processes in Plasmas* (Atomizdat, Moscow, 1968), Chapter 7.

[29] V. I. Vendeneyev, L. V. Gurvich, V. N. Kondrat'yev, V. A. Medvedev, and Ye L. Frankevich, *Bond Energies, Ionization Potentials, and Electron Affinities* (St. Martins Press, New York, 1966).

[30] S. J. Smith, in *Methods of Experimental Physics*, Vol. 7a, *Atomic and Electron Physics: Atomic Interactions*, B. Bederson and W. L. Fite, Eds. (Academic, New York, 1968), pp. 179–208.

[31] F. M. Page and G. C. Goode, *Negative Ions and the Magnetron*, (Wiley Interscience, New York, 1969); F. M. Page, Vacuum **24**, 523 (1974).

[32] R. S. Berry, Chemical Reviews **69**, 533 (1969).

[33] B. Steiner, in *Case Studies in Atomic Physics II*, E. W. McDaniel and M. R. C. McDowell, Eds. (North Holland, Amsterdam, 1972), pp. 485–545.

[34] J. L. Franklin and P. W. Harland, in *Annual Review of Physical Chemistry*, Vol. 25, H. Eyring, Ed. (Annual Reviews, Palo Alto, Calif., 1974), pp. 485–526.

[35] H.-P. Popp, Physics Reports **16**, 169 (1975); Vacuum **24**, 551 (1974).

[36] G. J. Schulz, Rev. Mod. Phys. **45**, 378 (1973).

[37] G. J. Schulz, Rev. Mod. Phys. **45**, 423 (1973).

[38] H. Baumann, E. Heinicke, H. J. Kaiser, and K. Bethge, Nucl. Instr. Meth. **95**, 389 (1971).

[39] J. E. Ahnell and W. S. Koski, Nature Phys. Sci. **245**, 30 (1973).

[40] W. C. Lineberger, A. Kasdan, and J. Carlsten (to be published).

[41] R. Rackwitz, Dissertation, Universität Hamburg, 1975.

[42] D. S. Walton, B. Peart, and K. T. Dolder, J. Phys. B **3**, L148 (1970).

[43] H. S. Taylor and L. D. Thomas, Phys. Rev. Lett. **28**, 1091 (1972).

[44] E. Clementi and A. D. McLean, Phys. Rev. **133**, A419 (1964).

[45] E. Clementi and C. Roetti, At. Data and Nucl. Data Tables (USA) **14**, 177 (1974).

[46] A. Veillard and E. Clementi, J. Chem. Phys. **49**, 2415 (1968).

[47] C. M. Moser and R. K. Nesbet, Phys. Rev. A **4**, 1336 (1971).

[48] C. M. Moser and R. K. Nesbet, Phys. Rev. A **6**, 1710 (1972).

[49] F. Sasaki and M. Yoshimine, Phys. Rev. A **9**, 26 (1974).

[50] E. Clementi, A. D. McLean, D. L. Raimondi, and M. Yoshimine, Phys. Rev. **133**, A1274 (1964).

[51] E. Clementi, Phys. Rev. **135**, A980 (1964).

[52] E. Clementi, J. Chem. Phys. **38**, 2248 (1963).

[53] E. Clementi, J. Chem. Phys. **39**, 175 (1963).

[54] J. Midtdal, Phys. Rev. **138**, 1010 (1965).

[55] J. Midtdal and K. Aashamar, Physica Norvegica **2**, 99 (1967).

[56] C. L. Pekeris, Phys. Rev. **112**, 1649 (1958).

[57] C. L. Pekeris, Phys. Rev. **126**, 1470 (1962).

[58] K. Aashamar, Nucl. Instrum. Meth. **90**, 263 (1970).

[59] A. W. Weiss, Phys. Rev. **122**, 1826 (1961).

[60] F. P. Schäfer, Ed., *Dye Lasers* (Springer Verlag, New York, Heidelberg, Berlin, 1974).

[61] A. W. Weiss, Phys. Rev. **166**, 70 (1968).

[62] A. C. Fung and J. J. Matese, Phys. Rev. A **5**, 22 (1972).

[63] N. Grün, Z. Naturforsch. **27a**, 843 (1972).

[64] L. Szasz, Acta Phys. Hung. **6**, 307 (1956).

[65] L. Szasz and G. McGinn, J. Chem. Phys. **56**, 1019 (1972).

[66] a) D. W. Norcross, Phys. Rev. Lett. **32**, 192 (1974).
     b) D. W. Norcross, private communication, 1974.

[67] L. Szasz, J. Chem. Phys. **49**, 679 (1968).

[68] W. H. E. Schwarz, Chem. Phys. Lett. **10**, 478 (1971).

[69] G. A. Victor and C. Laughlin, Chem. Phys. Lett. **14**, 74 (1972).

[70] C. Laughlin, R. F. Stewart, and G. A. Victor, *Fourth International Conference on Atomic Physics: Abstracts of Papers*, Heidelberg, July 22–26, 1974, pp. 158–159.

[71] P. Cavaliere, G. Ferrante, and R. Geracitano, Il Nuovo Cimento **9**, 96 (1972).

[72] J. N. Bardsley, Case Studies in Atomic Physics **4**, 302 (1974).

[73] A. Kancerevičius, *Fourth International Conference on Atomic Physics: Abstracts of Papers*, Heidelberg, July 22–26, 1974, pp. 150–153.

[74] Yu. F. Bydin, Zh. Eksp. Teor. Fiz. **46**, 1612 (1964) [Sov. Phys.-JETP **19**, 1091 (1964)].

[75] H. Ebinghaus, Z. Naturforsch. **19a**, 727 (1964).

[76] B. Ya'akobi, Phys. Letters **23**, 655 (1966).

[77] M. D. Scheer and J. Fine, J. Chem. Phys. **50**, 4343 (1969).

[78] H. Schmidt-Böcking and K. Bethge, J. Chem. Phys. **58**, 3244 (1973).

[79] H. Kaiser, E. Heinicke, R. Rackwitz, and D. Feldmann, Z. Physik **270**, 259 (1974).

[80] A. W. Weiss, Phys. Rev. A **3**, 126 (1971).

[81] M. A. Marchetti, M. Krauss, and A. W. Weiss, Phys. Rev. A **5**, 2387 (1972).

[82] H. F. Schaefer III and F. E. Harris, Phys. Rev. **170**, 108 (1968).

[83] H. F. Schaefer III and R. A. Klemm, J. Chem. Phys. **51**, 4643 (1969).

[84] İ. Öksüz and O. Sinanoğlu, Phys. Rev. **181**, 42 (1969).

[85] İ. Öksüz and O. Sinanoğlu, Phys. Rev. **181**, 54 (1969).

[86] P. S. Bagus, A. Hibbert, and C. Moser, J. Phys. B: Atom. Molec. Phys. **4**, 1611 (1971).

[87] F. Sasaki and M. Yoshimine, Phys. Rev. A **9**, 17 (1974).

[88] R. J. W. Henry, P. G. Burke, and A.-L. Sinfailam, Phys. Rev. **178**, 218 (1969).

[89] M. LeDourneuf and V. K. Lan, *Fourth International Conference on Atomic Physics: Abstracts of Papers*, Heidelberg, July 22-26, 1974, pp. 154-157.

[90] R. K. Nesbet, T. L. Barr, and E. R. Davidson, Chem. Phys. Lett. **4**, 203 (1969).

[91] T. Lee, N. C. Dutta, and T. P. Das, Phys. Rev. A **4**, 1410 (1971).

[92] N. C. Dutta and C. M. Dutta, Phys. Rev. A **6**, 959 (1972).

[93] G. Simons, J. Chem. Phys. **55**, 756 (1971).

[94] J. W. Viers, F. E. Harris, and H. F. Schaefer III, Phys. Rev. A **1**, 24 (1970).

[95] C. M. Moser and R. K. Nesbet, Phys. Rev. A **11**, 1157 (1975).

[96] G. Glockler, Phys. Rev. **46**, 111 (1934).

[97] B. Edlén, J. Chem. Phys. **33**, 98 (1960).

[98] M. Kaufman, Astrophys. J. **137**, 1296 (1963).

[99] A. P. Ginsberg and J. M. Miller, J. Inorg. Nucl. Chem. **7**, 351 (1958).

[100] J. W. Edie and F. Rohrlich, J. Chem. Phys. **36**, 623 (1962); Erratum: J. Chem. Phys. **37**, 1151 (1962).

[101] R. J. S. Crossley, Proc. Phys. Soc. **83**, 375 (1964).

[102] R. J. Zollweg, J. Chem. Phys. **50**, 4251 (1969).

[103] J. Hunt and B. L. Moiseiwitsch, J. Phys. B: Atom. Molec. Phys. **3**, 892 (1970).

[104] B. Edlén, in *Topics in Modern Physics*, W. E. Brittin and H. Odabasi, Eds. (Colorado Associated Univ. Press, Boulder, Colorado, 1971), pp. 133-145.

[105] B. Edlén, *Handbuch der Physik* (Springer-Verlag, Berlin, 1964), Vol. 27, pp. 79-220.

[106] H. R. Johnson and F. Rohrlich, J. Chem. Phys. **30**, 1608 (1959).

[107] M. A. Catalan, F. Rohrlich, and A. S. Shenstone, Proc. Roy. Soc. (London) **A221**, 421 (1954).

[108] E. C. Baughan, Trans. Faraday Soc. **57**, 1863 (1961).

[109] D. R. Bates and B. L. Moiseiwitsch, Proc. Phys. Soc. **A68**, 540 (1955).

[110] O. P. Charkin and M. E. Dyatkina, Zh. Strukt. Khim. **6**, 422 (1965) [J. Struct. Chem. (USSR) **6**, 397 (1965)].

[111] G. Glockler, J. Chem. Phys. **32**, 708 (1960).

[112] C. W. Scherr, J. N. Silverman, and F. A. Matsen, Phys. Rev. **127**, 830 (1962).

[113] A. G. Kamenev, E. Ya. Zandberg, and V. I. Paleev, Zh. Tekh. Fiz. **44**, 1507 (1974) [Sov. Phys. Tech. Phys. **19**, 940 (1975)].

[114] H. J. Kaiser, E. Heinicke, R. Rackwitz, and D. Feldmann, Verhandl. DPG (VI) **9**, 393 (1974); Spring Meeting, German Physical Society, Stuttgart, 1974; E. Heinicke, H. S. Kaiser, R. Rackwitz, and D. Feldmann, Phys. Lett. **50A**, 265 (1974).

[115] H. J. Kaiser, Dissertation, Ruprecht-Karl-Universitat Heidelberg, 1973.

[116] M. D. Scheer and J. Fine, Phys. Rev. Lett. **17**, 283 (1966).

[117] M. D. Scheer and J. Fine, J. Chem. Phys. **46**, 3998 (1967).

[118] M. D. Scheer, J. Res. Nat. Bur. Std. **74A**, 37 (1970).

[119] P. Politzer, Trans. Faraday Soc. **64**, 2241 (1968).

[120] V. B. Gohel and V. M. Trivedi, Indian J. Pure Appl. Phys. **10**, 474 (1972).

[121] K. P. Thakur, Indian J. Pure Appl. Phys. **11**, 549 (1973).

[122] L. M. Branscomb and W. L. Fite, Phys. Rev. **93**, 651A (1954).

[123] L. M. Branscomb and S. J. Smith, Phys. Rev. **98**, 1028 (1955).

[124] L. M. Branscomb and S. J. Smith, J. Chem. Phys. **25**, 598 (1956).

[125] L. M. Branscomb, D. S. Burch, S. J. Smith, and S. Geltman, Phys. Rev. **111**, 504 (1958).

[126] M. L. Seman and L. M. Branscomb, Phys. Rev. **125**, 1602 (1962).

[127] B. Steiner, M. L. Seman, and L. M. Branscomb, J. Chem. Phys. **37**, 1200 (1962).

[128] B. Steiner, M. L. Seman, and L. M. Branscomb, in *Atomic Collision Processes*, M. R. C. McDowell, Ed. (North-Holland, Amsterdam, 1964), pp. 537-542.

[129] R. A. Bennett and J. L. Hall, to be published.

[130] A. Kasdan, E. Herbst, and W. C. Lineberger, Chem. Phys. Lett. **31**, 78 (1975).

[131] B. Steiner, Phys. Rev. **173**, 136 (1968).

[132] B. Steiner, in *Sixth International Conference on the Physics of Electronic and Atomic Collisions: Abstracts of Papers* (MIT Press, Cambridge, Mass., 1969), pp. 535-537.

[133] D. Feldmann, Z. Naturforsch. **25a**, 621 (1970).

[134] D. Feldmann, Z. Naturforsch. **26a**, 1100 (1971).

[135] P. P. Sorokin and J. R. Lankard, IBM J. Res. Develop. **10**, 162 (1966).

[136] F. P. Schäfer, W. Schmidt, and S. Volze, Appl. Phys. Lett. **9**, 306 (1966).

[137] W. Demtröder, Physics Reports **5**, 223 (1973).

[138] W. Lange, J. Luther, and A. Steudel, in *Advances in Atomic and Molecular Physics*, Vol. 10, D. R. Bates and B. Bederson, Eds. (Academic, New York, 1974).

[139] C. B. Moore, Ed., *Chemical and Biochemical Applications of Lasers*, Vol. 1 (Academic, New York, 1974).

[140] E. P. Wigner, Phys. Rev. **73**, 1002 (1948).

[141] R. T. Hodgson, P. P. Sorokin, and J. J. Wynne, Phys. Rev. Lett. **32**, 343 (1974).

[142] S. E. Harris and R. B. Miles, Appl. Phys. Lett. **19**, 385 (1971); A. H. Kung, J. F. Young, and S. E. Harris, Appl. Phys. Lett. **22**, 301 (1974).

[143] D. M. Bloom, J. T. Yardley, J. F. Young, and S. E. Harris, Appl. Phys. Lett, **24**, 427 (1974).

[144] T. A. Patterson, Thesis, University of Colorado, 1974.

[145] J. I. Brauman and K. C. Smyth, J. Am. Chem. Soc. **91**, 7778 (1969).

[146] K. C. Smyth, R. T. McIver, Jr., J. I. Brauman, and R. W. Wallace, J. Chem. Phys. **54**, 2758 (1971).

[147] K. C. Smyth and J. I. Brauman, J. Chem. Phys. **56**, 1132 (1972).

[148] K. C. Smyth and J. I. Brauman, J. Chem. Phys. **56**, 4620 (1972).

[149] K. C. Smyth and J. I. Brauman, J. Chem. Phys. **56**, 5993 (1972).

[150] J. H. Richardson, L. M. Stephenson, and J. I. Brauman, Chem. Phys. Lett. **25**, 318 (1974); J. Chem. Phys. **62**, 1580 (1975).

[151] K. J. Reed and J. I. Brauman, J. Chem. Phys. **61**, 4830 (1974).

[152] R. S. Berry, C. W. Reimann, and G. N. Spokes, J. Chem. Phys. **37**, 2278 (1962).

[153] a) R. S. Berry and C. W. Reimann, J. Chem. Phys. **38**, 1540 (1963).
b) R. Milstein and R. S. Berry, J. Chem. Phys. **55**, 4146 (1971).

[154] R. S. Berry and C. W. David, in *Atomic Collision Processes*, M. R. C. McDowell, Ed. (North-Holland, Amsterdam, 1964), pp. 543-548.

[155] R. S. Berry, C. W. David, and J. C. Mackie, J. Chem. Phys. **42**, 1541 (1965).

[156] R. S. Berry, J. C. Mackie, R. L. Taylor, and R. Lynch, J. Chem. Phys. **43**, 3067 (1965).

[157] H.-P. Popp, Z. Naturforsch. **20a**, 642 (1965).

[158] H.-P. Popp, Z. Naturforsch. **22a**, 254 (1967).

[159] G. Mück and H.-P. Popp, Z. Naturforsch. **23a**, 1213 (1968).

[160] H. Frank, M. Neiger, and H.-P. Popp, Z. Naturforsch. **25a**, 1617 (1970).

[161] H. Hoffmann and H.-P. Popp, private communication; see also Verhandl. DPG (VI) **9**, 481 (1974); Spring Meeting, German Physical Society, Stuttgart, 1974.

[162] M. Neiger, Verhandl. DPG (VI) **9**, 481 (1974); Spring Meeting, German Physical Society, Stuttgart, 1974; M. Neiger, Dissertation, Electrophys. Inst. Tech. Univ. Munich, 1973; see also H.-P. Popp, ref. [35].

[163] G. Pietsch and L. Rehder, Z. Naturforsch. **22a**, 2127 (1967).

[164] D. E. Rothe, Phys. Rev. **177**, 93 (1969).

[165] P. M. Dehmer and W. A. Chupka, J. Chem. Phys. **62**, 4525 (1975).

[166] T. F. O'Malley, Phys. Rev. **137**, A1668 (1965).

[167] G. A. Kobzev, Zh. Eksp. Teor. Fiz. **61**, 582 (1971) [Sov. Phys.–JETP **34**, 310 (1972)].

[168] J. D. Morrison, H. Hurzeler, M. G. Inghram, and H. E. Stanton, J. Chem. Phys. **33**, 821 (1960).

[169] F. A. Elder, D. Villarejo, and M. G. Inghram, J. Chem. Phys. **43**, 758 (1965).

[170] V. H. Dibeler, J. A. Walker, and K. E. McCulloh, J. Chem. Phys. **51**, 4230 (1969).

[171] K. E. McCulloh and J. A. Walker, Chem. Phys. Lett. **25**, 439 (1974).

[172] W. A. Chupka and J. Berkowitz, J. Chem. Phys. **54**, 5126 (1971).

[173] J. Berkowitz, W. A. Chupka, P. M. Guyon, J. H. Holloway, and R. Spohr, J. Chem. Phys. **54**, 5165 (1971).

[174] J. Berkowitz, W. A. Chupka, and T. A. Walter, J. Chem. Phys. **50**, 1497 (1969).

[175] P. J. Chantry and G. J. Schulz, Phys. Rev. **156**, 134 (1967).

[176] W. R. Henderson, W. L. Fite, and R. T. Brackmann, Phys. Rev. **183**, 157 (1969).

[177] R. N. Il'in, in *Atomic Physics 3*, Proceedings of the Third International Conference on Atomic Physics, August 7–11, 1972, Boulder, Colorado, S. J. Smith and G. K. Walters, Eds. (Plenum Press, New York, 1973), pp. 309–26.

[178] B. M. Smirnov and M. I. Chibisov, Zh. Eksp. Teor. Fiz. **49**, 841 (1965) [Sov. Phys.–JETP **22**, 585 (1966)].

[179] A. C. Riviere and D. R. Sweetman, Phys. Rev. Lett. **5**, 560 (1960).

[180] V. A. Oparin, R. N. Il'in, I. T. Serenkov, E. S. Solov'ev, and N. V. Fedorenko, ZhETF Pis. Red. **12**, 237 (1970) [JETP Lett. **12**, 162 (1970)].

[181] É. Ya. Zandberg and N. I. Ionov, Usp. Fiz. Nauk. **67**, 581 (1959) [Sov. Phys. Usp. **2**, 255 (1959)].

[182] I. N. Bakulina and N. I. Ionov, Dokl. Akad. Nauk SSSR **155**, 309 (1964) [Sov. Phys. Dokl. **9**, 217 (1964)].

[183] É. Ya. Zandberg and V. I. Paleev, Dokl. Akad. Nauk SSSR **190**, 562 (1970) [Sov. Phys. Dokl. **15**, 52 (1970)].

[184] É. Ya. Zandberg, A. G. Kamenev, and V. I. Paleev, Zh. Tekh. Fiz. **41**, 1057 (1971) [Sov. Phys. – Tech. Phys. **16**, 832 (1971)].

[185] É. Ya. Zandberg, A. G. Kamenev, and V. I. Paleev, Zh. Tekh. Fiz. **41**, 1983 (1971) [Sov. Phys. – Tech. Phys. **16**, 1567 (1972)].

[186] E. Ya. Zandberg and V. I. Paleev, Zh. Tekh. Fiz. **42**, 844 (1972) [Sov. Phys. – Tech. Phys. **17**, 665 (1972)].

[187] É. Ya. Zandberg, A. G. Kamenev, and V. I. Paleev, Zh. Tekh. Fiz. **44**, 617 (1974) [Sov. Phys. – Tech. Phys. **19**, 385 (1974)];

É. Ya. Zandberg, Zh. Tekh. Fiz. **44**, 1809 (1974) [Sov. Phys. – Tech. Phys. **19**, 1133 (1975)].

[188] R. E. Honig, J. Chem. Phys. **22**, 126 (1954).

[189] F. M. Page, Trans. Faraday Soc. **56**, 1742 (1960).

[190] F. M. Page, Trans. Faraday Soc. **57**, 359 (1961).

[191] D. A. Ansdell and F. M. Page, Trans. Faraday Soc. **58**, 1084 (1962).

[192] Yu. F. Bydin, Zh. Eksp. Teor. Fiz. **49**, 1094 (1965) [Sov. Phys.–JETP **22**, 762 (1966)].

[193] O. B. Firsov, Sov. Phys.–JETP **21**, 1001 (1951).

[194] R. N. Compton and C. D. Cooper, J. Chem. Phys. **59**, 4140 (1973).

[195] C. D. Cooper and R. N. Compton, J. Chem. Phys. **60**, 2424 (1974).

[196] R. N. Compton, P. W. Reinhardt, and C. D. Cooper, J. Chem. Phys. **60**, 2953 (1974).

[197] C. Lifshitz, B. M. Hughes, and T. O. Tiernan, Chem. Phys. Lett. **7**, 469 (1970).

[198] T. O. Tiernan, B. M. Hughes, and C. Lifshitz, J. Chem. Phys. **55**, 5694 (1971).

[199] C. Lifshitz, T. O. Tiernan, and B. M. Hughes, J. Chem. Phys. **59**, 3182 (1973).

[200] L. M. Blau, R. Novick, and D. Weinflash, Phys. Rev. Lett. **24**, 1268 (1970).

[201] D. L. Mader and R. Novick, in *Atomic Physics 3*, S. J. Smith and G. K. Walters, Eds. (Plenum, New York, 1973), pp. 169–180.

[202] E. Holøien and S. Geltman, Phys. Rev. **153**, 81 (1967).

[203] K. Bethge, E. Heinicke, and H. Baumann, Phys. Lett. **23**, 542 (1966).

[204] V. A. Oparin, R. N. Il'in, I. T. Serenkov, E. S. Solov'ev, and N. V. Fedorenko, ZhETF Pis. Red. **13**, 351 (1971) [JETP Lett. **13**, 249 (1971)].

[205] Ya. M. Fogel', V. F. Kozlov, and A. A. Kalmykov, Zh. Eksp. Teor. Fiz. **36**, 1354 (1959) [Sov. Phys.–JETP **36**, 963 (1959)].

[206] G. E. Norman, Opt. Spectrosc. **17**, 94 (1964).

[207] Yu. V. Moskvin, Opt. Spectrosc. **27**, 356 (1970).

[208] G. Boldt, Z. Physik **154**, 330 (1959).

[209] J. C. Morris, R. U. Krey, and R. L. Garrison, Phys. Rev. **180**, 167 (1969).

[210] D. Feldmann, private communication.

[211] W. A. Chupka, D. Spence and C. M. Stevens, in Argonne National Laboratory Report ANL–75–3 (1975), p. 126.

[212] W. C. Lineberger and J. Slater, Abstracts, IX ICPEAC, Seattle, Wash., July, 1975.

[213] P. D. Burrow and J. A. Michejda, Proc., Internat'l. Symp. on Electron and Photon Interactions with Atoms, Stirling, Scotland, 1974, p. 50.

[214] E. R. Cohen and B. N. Taylor, J. Phys. Chem. Ref. Data **2**, 663 (1973).

[215] R. A. Bennett, Thesis, University of Colorado, 1972.

[216] V. McKoy and O. Sinanoğlu, in *Modern Quantum Chemistry, Part II: Interactions*, O. Sinanoğlu, Ed. (Academic, New York, 1965), pp. 23–32.

[217] V. McKoy and O. Sinanoğlu, J. Chem. Phys. **41**, 2689 (1964).

[218] P. G. Burke, K. A. Berrington, M. LeDourneuf, and Vo Ky Lan, J. Phys. B **7**, L531 (1974).

[219] D. Feldmann, Phys. Lett. **53A**, 82 (1975).

[220] P. M. Dehmer and W. A. Chupka, Bull. Am. Phys. Soc. **20**, 729 (1975).

[221] D. R. Herrick and F. H. Stillinger, J. Chem. Phys. **62**, 4360 (1975).

[222] P. D. Burrow and J. Comer, J. Phys. B **8**, L92 (1975).